AD-A048 889 OHIO STATE UNIV COLUMBUS DEPT OF GEODETIC SCIENCE F/G 8/5
NON-STATIONARY ESTIMATION IN GRAVITY PREDICTION PROBLEMS.(U)
JUL 77 W KEARSLEY F19628-77-C-0082
UNCLASSIFIED DGS-256 AFGL-TR-77-0186 NL

| OF |
AD
AD48889

END
DATE
FILMED
2-78
DDC

AFGL-TR-77-0186

NON-STATIONARY ESTIMATION IN GRAVITY PREDICTION PROBLEMS

William Kearsley

The Ohio State University
Research Foundation
Columbus, Ohio 43212

July 1977

Scientific Report No. 1

AIR FORCE GEOPHYSICS LABORATORY
AIR FORCE SYSTEMS COMMAND
UNITED STATES AIR FORCE
HANSCOM AFB, MASSACHUSETTS 01731

Unclassified

SECURITY CLASSIFICATION OF THIS PAGE (When Data Entered)

(19) REPORT DOCUMENTATION PAGE	READ INSTRUCTIONS BEFORE COMPLETING FORM
(18) 1. REPORT NUMBER: AFGL-TR-77-0186	2. GOVT ACCESSION NO. / 3. RECIPIENT'S CATALOG NUMBER (9)
(6) 4. TITLE (and Subtitle): NON-STATIONARY ESTIMATION IN GRAVITY PREDICTION PROBLEMS,	5. TYPE OF REPORT & PERIOD COVERED: Scientific. Interim rept. Scientific Report No. 1
	6. PERFORMING ORG. REPORT NUMBER: Geodetic Science No. 256 ✓
(10) 7. AUTHOR(s): William Kearsley	8. CONTRACT OR GRANT NUMBER(s): (15) F19628-77-C-0082 new ✓
9. PERFORMING ORGANIZATION NAME AND ADDRESS: Department of Geodetic Science, The Ohio State University - 1958 Neil Avenue, Columbus, OH 43210	10. PROGRAM ELEMENT, PROJECT, TASK AREA & WORK UNIT NUMBERS: 61102F (16) 2309G1AB (17) G1
11. CONTROLLING OFFICE NAME AND ADDRESS: Air Force Geophysics Laboratory, Hanscom AFB, Mass. 01731, Contract Monitor: Bela Szabo/LW	(11) 12. REPORT DATE: Jul[redacted]77
	13. NUMBER OF PAGES: (12) 63 p.
14. MONITORING AGENCY NAME & ADDRESS(if different from Controlling Office): (14) DGS-256, Scientific-1	15. SECURITY CLASS. (of this report): Unclassified
	15a. DECLASSIFICATION/DOWNGRADING SCHEDULE

16. DISTRIBUTION STATEMENT (of this Report)

A-Approved for public release; distribution unlimited

17. DISTRIBUTION STATEMENT (of the abstract entered in Block 20, if different from Report)

18. SUPPLEMENTARY NOTES

19. KEY WORDS (Continue on reverse side if necessary and identify by block number)

Least squares prediction, collocation, isotropy, covariance functions.

20. ABSTRACT (Continue on reverse side if necessary and identify by block number)

This report investigates the impact that the assumptions of homogeneity and isotropy, when applied to potential related fields, have upon the stochastic processes which are applied to these fields. After seeing how these assumptions are incorporated into the statistical model to produce the familiar covariance function, the investigation centers on techniques which can be used to detect the presence of anisotropy in the field. The method found most useful in the two-

DD FORM 1 JAN 73 1473 EDITION OF 1 NOV 65 IS OBSOLETE

400254

Unclassified

SECURITY CLASSIFICATION OF THIS PAGE (When Data Entered)

dimensional covariance function, and some methods of representing this function are also investigated.

Numerical studies are then carried out to see the effect the use of the 2-D covariance function has upon the results of prediction and collocation computations. It is found that, under certain circumstances, the 2-D function produces a result superior to that given by the general function. Recommendations are then given as to when the 2-D covariance function should be used in practical solutions, and suggestions made as to the possible areas of further research.

Foreword

This report was prepared by Dr. William Kearsley, Research Associate, Department of Geodetic Science, The Ohio State University, under Air Force Contract No. F19628-77-C-0082, The Ohio State University Research Foundation Project No. 710534, which is under the direction of Professor Richard H. Rapp. The contract covering this research is administered by the Air Force Geophysics Laboratory, Hanscom Air Force Base, Massachusetts, with Mr. Bela Szabo, Contract Monitor.

Table of Contents

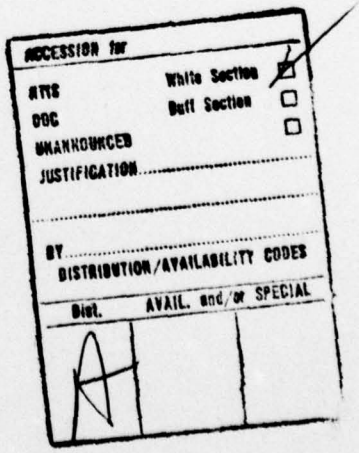

1. Introduction

The collocation method is now widely accepted and has been used to solve many geodetic problems, e.g. the computation of geoidal undulations and deflections of the vertical (Tscherning, 1973; Tscherning and Rapp, 1974; Lachapelle 1975a and 1975b) as well as for the extension of the gravity field from satellite altimetry (Rapp, 1974 and 1976). In its narrower and original form this technique has been used for the prediction of point or mean anomalies from the known gravity field (Rapp, 1964). In fact, the method has been used, at least experimentally, to assist in the solution of all aspects of the geodetic problem.

The covariance function is basic to collocation methods. This fact is emphasized by Moritz in his important work on the theory of collocation when he comments that, "Not only conceptually, but also computationally the covariances represent the crucial point in the present method..." (Moritz, 1972, p. 21). These functions are meant to represent the statistical characteristics of the fields they represent, and in their derivation conditions of homogeneity and isotropy are assumed to exist in the fields. It is the correctness of this assumption which is being investigated here; if the assumptions are found to be inaccurate it will be necessary to assess the impact that the lack of accuracy has on the method, and to suggest ways of modifying the method to account for an 'improved' model.

Although the covariance functions of the anomalous potential field is the theoretical basis for covariance functions of other (potential-related) fields (Jordan, 1972; Moritz, 1972, p. 94-99) it is usual for the Δg field to form the basis for most collocation solutions (e.g. Lachapelle, 1975a, p. 23-24). For this reason this investigation will at first concentrate on the detection of anisotropy in anomalous gravity fields. This is then extended to the behavior of cross-covariance functions and the effects of using an isotropic model for collocation in an anisotropic region are investigated.

The assumption of an homogeneous gravity field throughout the globe has been queried for as long as covariance techniques have been discussed. For example, Rapp investigated three different regions of the United States and found significantly different covariance functions for each from the analysis of these fields (Rapp, 1964, p. 42-65). Williamson and Gaposhkin analyzed subsets of data of ocean and continental gravity assuming isotropy, and found the differences between the covariances to be significant. They concluded that "...gravity is not stationary" (Gaposhkin, 1973, p. 208). Similarly, in a statistical analysis of anomalous gravity of Czechoslovakia, Vyskočil (1970) investigated the covariance functions for Δg means of 10' x 15' blocks and concluded "the theoretical assumption of homogeneity and isotropy... is basically only forced and in reality it will probably not always be satisfied." (See also Kaula, 1966b, p. 58.)

It is common practice to allow for the non-homogeneity of the gravity field by restricting the analysis to that data pertinent to the area of solution. That is, a local covariance function based on a restricted gravity field is derived and used in subsequent computations for that area. The problem remaining is how to test such a local field for isotropy and, if characteristics of non-isotropy are exhibited, how to include these in the computations.

As already mentioned, Vyskočil (qv) has expressed concern that non-isotropy can exist. A comparison of the profile analysis by Rapp (1964, p. 44-56) shows large differences between N-S and E-W profiles of the same area, casting doubt on the assumption that the covariance functions are independent of azimuth. Kubáčková (1974) has studied the gravity field in the Carpathian Mountains of Czechoslovakia, and concludes that the departure from a situation of isotropy is not insignificant, suggesting that use of a covariance function based on an isotropic model "is impermissible without prior analysis of the consequences."

The purpose of this report is threefold. Firstly, it is to see how anisotropic characteristics in a data field are best detected and portrayed. Secondly, to find out if an anisotropic model can be introduced into the theory of prediction and collocation. Lastly, we wish to investigate if an 'improved' statistical model produces any significant effect on the results of prediction and collocation solutions.

It may be that such improvement is marginal. It has already been pointed out that "...the choice of the covariance function is less critical (i.e. than internal consistency in the computations - author's note) because the results of least squares collocation are not very sensitive with respect to the covariance function chosen, in the same way that the results of ordinary least squares adjustment do not depend strongly on the weights" (Moritz, 1972, p. 90). Tukey (1970, p. 165-166) estimates that in ordinary least squares situations, if the ratio of each true weight to the weight you use does not vary by more than a factor of 2, then the efficiency of the fit is always at least 88.8%. However, he then differentiates between the normal least squares solution and the time-series situation, pointing out that due to the overlap in data, some bias will result if the variances and covariances are incorrectly estimated.

"When in doubt, smooth" (Moritz, 1972, p. 125) is a valuable and useful maxim, but there may be cases where such a procedure is contrary to a preliminary appreciation of the situation. It may be that to 'smooth' without fully establishing the 'doubt' is detrimental to the resultant solution.

2.0 The Theoretical Background

2.1 The Covariance Function

The application of covariance analysis to gravimetric geodesy is well known (Heiskanen and Moritz, 1967, 252-259, 266-274). The fundamentals will be briefly reviewed here in order to emphasize how the assumption of randomness of the gravity field influences the mathematical representation of its covariance function.

"The covariance characterizes the statistical correlation of the two signals, Δg and Δg_x, which is their tendency to have the same size and sign. If the covariance is zero then the anomalies Δg and Δg_x are uncorrelated i.e. the size and sign of Δg has no influence on the size and sign of Δg_x"(Ibid, 253).

This correlation is estimated by taking the mean of all product pairs throughout the globe, thus:

$$(2.1) \qquad C(P,Q) = \frac{1}{8\pi^2} \int_{\lambda=0}^{2\pi} \int_{\theta=0}^{\pi} \int_{\alpha=0}^{2\pi} \Delta g(\theta_P, \lambda_P)\, \Delta g(\theta_Q, \lambda_Q) \sin\theta \, d\theta \, d\lambda \, d\alpha$$

where

P, Q represent the current points in the product pair, ψ_{PQ} apart
θ, λ are the spherical coordinates of these points, and
α is the azimuth from P to Q.

If isotropy is assumed the covariance is independent of azimuth, and (2.1) becomes:

$$(2.2) \qquad C(P,Q) = \frac{1}{4\pi} \int_{\lambda=0}^{2\pi} \int_{\theta=0}^{\pi} \Delta g_P\, \Delta g_Q \sin\theta \, d\theta \, d\lambda$$

If homogeneity is assumed the covariance is independent of location on the globe, and since:

$$(2.3) \qquad \frac{1}{4\pi} \int_{\lambda=0}^{2\pi} \int_{\theta=0}^{\pi} \sin\theta \, d\theta \, d\lambda = \frac{1}{4\pi} \iint_{\sigma} d\sigma$$

(2.2) becomes a function of separation only. Thus:

$$(2.4) \qquad C(P,Q) = \frac{1}{4\pi} \iint_{\sigma} \Delta g_P\, \Delta g_Q \, d\sigma$$

If local regions are considered, the reference model can be assumed planar and the separation expressed as the straight line distance r_{PQ}, where:

(2.5) $$C(r) = M\left\{\Delta g_P, \Delta g_Q\right\} = C_{PQ}$$

$M\left\{x\right\}$ being the mean value of x.

For $r = 0$

(2.6) $$C_0 = C(0) = M\left\{\Delta g^2\right\}$$

the variance of the gravity anomalies. Note also that:

(2.7) $$M\left\{\Delta g\right\} = 0$$

which, if not the case, must be enforced by "centering" the data before commencing the analysis (see Rapp, 1964, p. 7 - 8).

In a local area the means of product pairs are usually computed from point data or from means of small areas (e.g. $0^\circ.1 \times 0^\circ.1$) arranged on a grid pattern. If the field is isotropic, the values of the means for any one separation are independent of azimuth. Conversely, if the means are computed without reference to azimuth (see equation 2.2) the property of isotropy is enforced onto the field.

An analytical function can be fitted to the values of C (r) (e.g. Moritz, 1976, p. 25 - 29). This function is a convenient way to generate the elements of the matrices used in subsequent computations. However, this fitting will have probably introduced further "smoothing" into the covariance function; thus the price paid for convenience may be a loss of precision in the representation of the statistical relationships between two points in the subject data field.

A review of the process will underline the stages at which the actual covariance may have undergone change. The covariance function has been found by:

(i) taking the means of product pairs throughout the region being analyzed,

(ii) taking the means regardless of the directional relationships of successive point pairs, and

(iii) fitting an analytical function to the resultant discrete field.

If homogeneity is present, the smoothing introduced by (i) will be minimal. If isotropy exists, step (ii) will also introduce a minimum of smoothing. If both conditions are present, then the function obtained in (iii) will accurately reflect the existing situation. How the covariance function is used will be demonstrated in the following section.

2.2 Least Squares Prediction

This discussion will concentrate on the application of stochastic methods in the prediction of gravity anomalies. This will assist in the appreciation of the stochastic techniques generally, and in particular will underline how the assumption of isotropy in the data field carries through into the formulation and solution of the problem. The more involved multivariate case will be treated separately (see section 2.4).

The covariance relationship is used in the determination of the coefficients a_{pi} of a univariate Kolmogorov-Wiener prediction model (Grafarend and Offermans, 1975, 3; Grafarend, 1976, p.152). Thus:

$$\Delta g'_p = \sum_i a_{pi}\, \Delta g_i \qquad i = 1, n \tag{2.8}$$

$\Delta g'_p$ being the predicted value of Δg at P.

The error of prediction is found, thus:

$$\epsilon_p^2 = (\Delta g_p - \sum_i a_{pi}\, \Delta g_i)^2 \tag{2.9}$$

These squared errors are now averaged through the region for all points P. Thus:

$$M\left\{\epsilon_p^2\right\} = M\left\{\Delta g_p^2\right\} - 2\sum_i a_{pi}\, M\left\{\Delta g_p\, \Delta g_i\right\} + \sum_i \sum_j a_{pi}\, a_{pj}\, M\left\{\Delta g_i\, \Delta g_j\right\} \tag{2.10}$$

$i = 1, n$
$j = 1, n$

Assuming that:

(2.11a) $$M\left\{\Delta g_p^2\right\} = M\left\{\Delta g_i^2\right\}$$

(2.11b) $$M\left\{\Delta g_p\, \Delta g_i\right\} = M\left\{\Delta g_i \Delta g_j\right\} \quad \text{for } r_{ij} = r_{pi}$$

and using the covariance function derived in section (2.1), (2.10) becomes:

(2.12) $$m_p^2 = C_0 - 2\sum_i a_{pi}\, C_{pi} + \sum_i \sum_j a_{pi}\, a_{pj}\, C_{ij}$$

where

(2.13) $$m_p^2 = M\left\{\epsilon_p^2\right\}$$

Note the approximations in (2.11). The values for Δg_p are (obviously) unknown, and so some assumption regarding their statistical relationship with respect to known values (Δg_i) must be made for (2.10) to be solveable. The accuracy of the estimates made in (2.11) will depend on:

(i) how well the characteristics of homogeneity and isotropy describe the actual Δg field, and

(ii) the amount of data used to find the C_0, C_{pi} and C_{ij} values.

This second point is fairly obvious and not of direct concern at the moment. It is sufficient to say that if the data is sparse, then a poor estimate for the covariance function is likely. This is despite any indications of good accuracy obtained from an estimate of internal precision (see section 2.3).

The first point is of more importance in this present discussion. If the field is well modelled by a stationary statistical model, then the approximations for $M\left\{\Delta g_p^2\right\}$ and $M\left\{\Delta g_p\, \Delta g_i\right\}$ will be realistic. Otherwise, these approximations are "smoothing" the real situation and characteristics of homogeneity and isotropy are imposed onto the predicted field.

The coefficients a_{pi} in equation (8) are now solved in the usual way by least squares, viz.

$$\frac{\partial(m_p^2)}{\partial a_{pi}} = 0 .$$

Thus it is found that:

$$a_{pj} = \sum_i C_{ij}^{-1} C_{pj} \qquad j = 1, n . \tag{2.14}$$

The predicted value is found by substitution of (2.14) into (2.8). Thus it can be seen how the adopted statistical model is imposed (by way of C_{ij} and C_{pi}) onto the predicted values for Δg_p .

2.3 Accuracy of Least Squares Prediction

The investigation is carried into the estimation of accuracy to help emphasize the role which the statistical model plays in this phase of the development.

Equation (2.9) can be used as the starting point; thus:

$$\epsilon_p = \Delta g_p - \sum a_{pi} \Delta g_i \tag{2.15}$$

where a_{pi} are found from (2.14). In equation (2.15) we are comparing the predicted value of Δg_p with Δg_p assumed known.

The procedure described in section (2.2) to find the mean square errors is again followed and it is found that:

$$m_p^2 = C_0 - C_{pi}^T C_{ij}^{-1} C_{pj} . \tag{2.16}$$

(In (2.16) matrix notation is used to simplify the expression). It must be noticed that estimates (2.11a) and (2.11b) are again used. The errors being determined are therefore not those at the unknown points P but at known points i. That is, equation (2.16) is a measure of the "fit" of a stationary statistical model onto the known data. (See also Grafarend, 1976, p. 154.)

This is an important distinction to make. While m_p^2 is probably a useful guide to the accuracy of the predicted values, it is strictly a measure of

the "fitness of the model". As such, it will be useful when comparing predictions based on anisotropic models with those using isotropic models (see section 4.1).

From the above comments one can see the danger in placing too much confidence on estimates of m_ρ^2 which are derived from small populations of data points. Because of the small number of constraints available in such cases, the solution will not be greatly overdetermined and will, in fact, approach a unique solution.

In fact, to obtain an alternative estimate of accuracy, one can carry out a simple error analysis on the original observation equation (2.8). In this approach the errors in the data can be found from a knowledge of the methods used to obtain the known Δg's (Brovar et al, 1964, p. 278-279; Kearsley, 1976, p. 120-122). The errors in the covariances could be estimated by statistical analysis of C_{ij} in the course of the evaluation of the covariance function (Ibid, p. 98-100).

2.4 Collocation Theory

In collocation, one predicts signals from observed data which are not necessarily of the same type as the signal predicted. For this, auto-correlations and cross-correlations are needed. It is also possible to incorporate in the technique the determination of parameters of a geometrical model which is chosen a priori in order to reduce systematic effects which may be present in the data.

The generalized observation equation of collocation is stated as:

$$x = AX + s' + n \tag{2.17}$$

where

- x is the measurement (e.g. gravity)
- AX defines a mathematical model (e.g. normal ellipsoid)
- s' is the signal (e.g. gravity anomaly), and
- n is the noise (e.g. measuring error in gravity)

Following the development by Moritz (1972, p. 7-16), the model parameters X are found by least squares to be:

$$X = (A^T \bar{C}^{-1} A)^{-1} A^T \bar{C}^{-1} x \tag{2.18}$$

and the predicted signals by:

$$s = C_{sx}\,\bar{C}^{-1}\,(x - AX) \tag{2.19}$$

where

$\bar{C} = C_{xx}$, the auto-covariance matrix of observations
C_{sx} = the cross-covariance matrix between signal and observed data.

It is noted that the expression which determines the model parameters is dependent on $\bar{C}$ and thus may be influenced by the choice of stochastic model. In the local context the model effects are generally removed by adopting parameters deduced from a "higher" (or global) solution. The problem then reduces to a "multivariate" prediction (Grafarend and Offermans, 1975, p. 4), where the task is to predict one potential-related parameter (e.g. N or ξ, η) from a second (e.g. Δg). It is this situation which is of concern in this present investigation.

As can be seen from (2.19) the prediction is a function of both the auto-covariances of the observed quantities, and the cross-covariances of the observed quantity with the predicted quantity. Both of these quantities are derived from the anomalous potential, and their covariance functions are thus indirectly related (Moritz, 1972, p. 94-99; Grafarend and Offermans, 1975, p. 28). A number of models have been suggested as suitable for representing the auto- and cross-covariance functions, both on a global scale (Tscherning and Rapp, 1974) and for the local case (Jordan, 1972). However, isotropy of the potential field and hence of the Δg field (Ibid, p. 3664) is usually assumed. (See also Grafarend and Offermans, 1975, p. 20-22; Grafarend, 1976, p. 164-165).

Thus it will be seen that the values resulting from (2.19) will have the characteristics of isotropy imposed on them by means of the auto- and cross-covariance functions. It is possible to include an azimuth term in the functions to account for anisotropy (Jordan, 1972, p. 3663). The situation is much more difficult to model (see section 4.3) due to complications which occur in the cross-covariances of two different signals. Nevertheless, it is obvious that the adoption of an isotropic statistical model to generate covariances in a non-isotropic region, while simplifying the solution, will cause smoothing which may be detrimental to the solution.

2.5 Comments

The methods of least squares collocation and prediction are often described as the "optimal" solutions of their respective problems given the data available (Heiskanen and Moritz, 1967, p. 269; Moritz, 1972, p. 18; Lachapelle, 1975a, p. 19). From this it has been inferred that the techniques as formulated provide the "best possible" method of predicting or solving for unknown parameters. Such a claim must be viewed in the light of the assumptions made in equations (2.2) and (2.11). If a stochastic model with properties of homogeneity and isotropy is not a good description of the actual field then a solution based upon this model will not necessarily give the most accurate solution. In other words, least squares prediction or collocation will give the optimal solution for the particular stochastic model adopted; whether or not this is the best of all solutions is dependent upon the faithfulness of this model to the real situation.

The matter as to whether or not a more sophisticated covariance model will have any practical impact on the solution has already been touched on in section 1. It is hoped that this investigation will provide some further insights into this question.

3. The Detection and Representation of Anisotropic Characteristics

3.1 Introduction

In this chapter various methods tested as a means of detecting anisotropy are reviewed. Possible ways of representing the azimuth-dependence of the statistical relationships are also suggested, it being realized that the method which is most efficient in detecting anisotropy will also provide the best foundation for its representation.

To aid in the appreciation of the methods, tests were carried out on a number of data sets, details of which appear in Table 1. Because of the limited extent of the data, it was safe to assume plane relationships existed between data points involved in the analysis.

Table 1

Details of Test Data Sets

Data Set No.	Location	Description	Data
1	$38° \leq \varphi \leq 39°$ $-83° \geq \lambda \geq -84°$	Strong ridge (wavelength $\simeq$ 30'; amplitude $\simeq$ 40 mgals) dominating on azimuth of 20° Range 80mgal (see Figure 1)	Free-air anomalies interpolated from isogal map on 5' grid interval
2	Generated Data	Sloping plane Max. 50mgal, SE corner Min. -2.5mgal, NW cnr. Azimuth of strike $\simeq$ 35°	As above
3	Generated Data	Sloping plane Max. 28mgal, E boundary Min. 2mgal, W boundary Azimuth of strike 0°	As above
4	$38° \leq \varphi \leq 39°$ $-82° \geq \lambda \geq -83°$	Flat, featureless Range 40 mgal Note: adjoins data set 1 (See Figure 2)	As above

Special attention must be paid to the dimensions of the grid in any procedure which attempts to analyze a continuous field represented by discrete points at grid intersections. The reader is referred to Blackman and Tukey (1959, 117-120), Horton et. al. (1964, 590-591) and Nettleton (1976, 159) for a discussion on this topic. In this particular case the 5' grid intersection was chosen as giving adequate representation in an already smoothened field. In most cases the maximum 'lag' or step (r in equation 2.5) was limited to half the number of data points in each row or column. The minimum sample size was approximately 50. In subsequent analyses the r. m. s. error of the mean obtained for this maximum step did not differ significantly from that for the initial step sizes, and so was considered a good estimate for the quantity being determined here (eg. the covariance, coskewance, etc.)

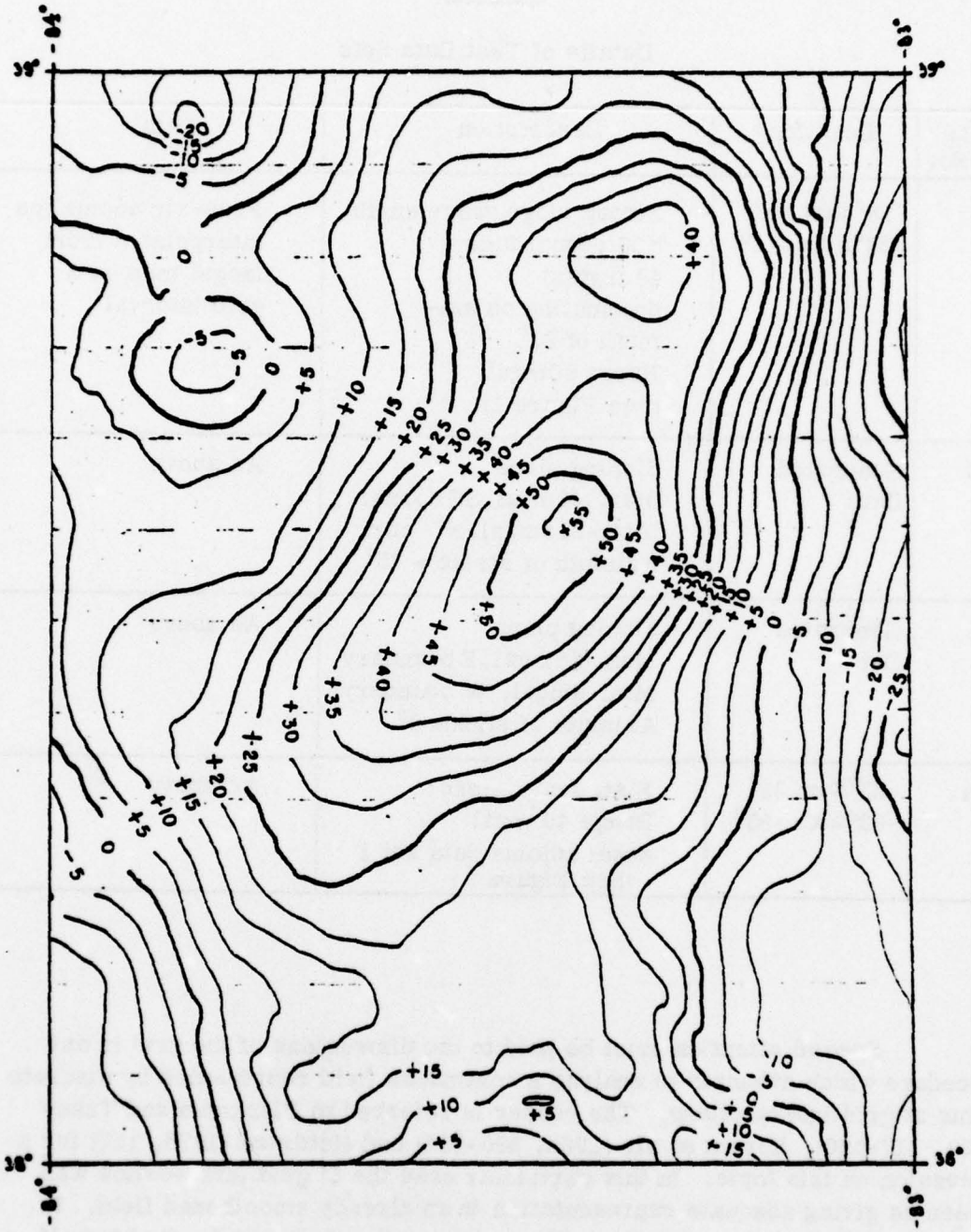

Figure 1. Free-air Gravity Anomalies - Data Set 1
(Contour Interval: 5 mgal)

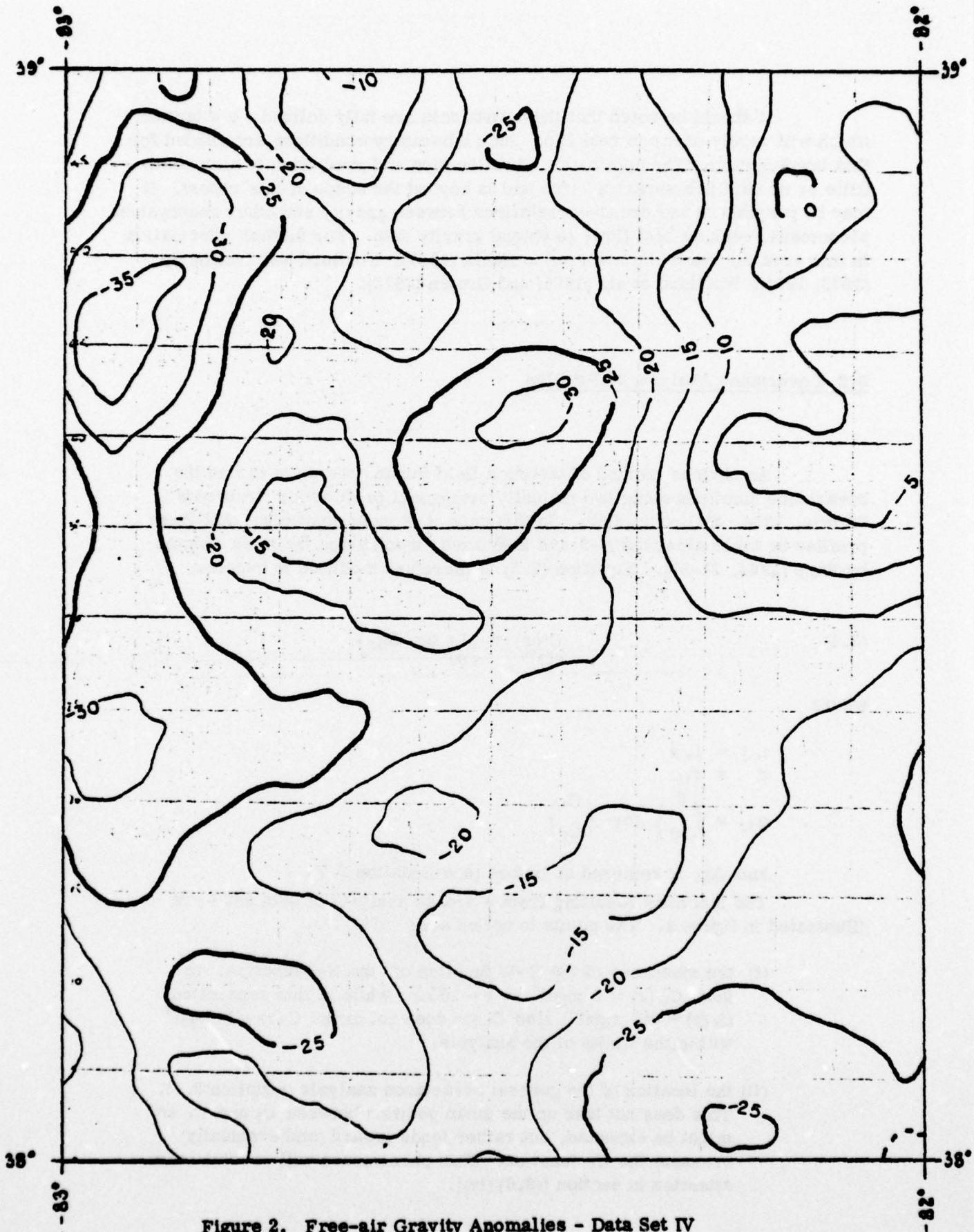

Figure 2. Free-air Gravity Anomalies - Data Set IV
(Contour Interval: 5 mgal)

It should be noted that these data sets are fully defined - a situation which will rarely occur in real life. Such laboratory conditions are needed for this investigation. The application of collocation and prediction in areas with little or no data is a separate issue and is beyond the scope of this report. It may be possible to use cross-correlations between gravity and other geophysical phenomena, such as heat flow, to extend gravity data. For further information in this area the reader is referred to Kaula (1967), Woollard and Daugherty (1970; 1974), Woollard et al. (1975) and Groten (1975).

3.2 Covariance Analysis of Profiles

An obvious method of testing a field for anisotropy is to find the covariance functions along two mutually orthogonal profiles (or 'transects', Whittle, 1954, 434) of the field. In this case it is most convenient that these profiles be taken along the N-S and E-W axes, much along the lines adopted by Rapp (1964, 31-57). Equation (2.5) is therefore modified to become:

$$(3.1) \qquad \underset{N(\alpha)}{C}(r) = \underset{N(\ell)}{M}\left\{\Delta g_i \, \Delta g_j\right\}$$

where

$$i, j = 1, n$$
$$r = r_{ij}$$
$$\alpha_{ij} = \begin{Bmatrix} 0 \\ 90 \end{Bmatrix} \text{ for } \begin{Bmatrix} C_N \\ C_\ell \end{Bmatrix}$$

and Δg_i is centered as before (see Equation 2.7).

The functions resulting from a profile analysis of data set 1 are illustrated in figure 3. The points to notice are:

(i) the steepness of the E-W function cf. the N-S function. In fact, $C_\ell(r) = 0$ mgal^2 at $r \simeq 30$ km, while at this separation $C_N(r) \simeq 260$ mgal^2; also $C_N(r)$ does not cross $C(r) = 0$ mgal^2 within the limits of the analysis.

(ii) the location of the general covariance analysis (equation 2.5). This does not take up the mean position between C_N and C_ℓ as might be expected, but rather tends toward (and eventually crosses) the C_ℓ function. This phenomenon will receive more attention in section [(3.6)(iv)].

FIGURE 3 : COVARIANCE FUNCTIONS FOR TEST DATA 1

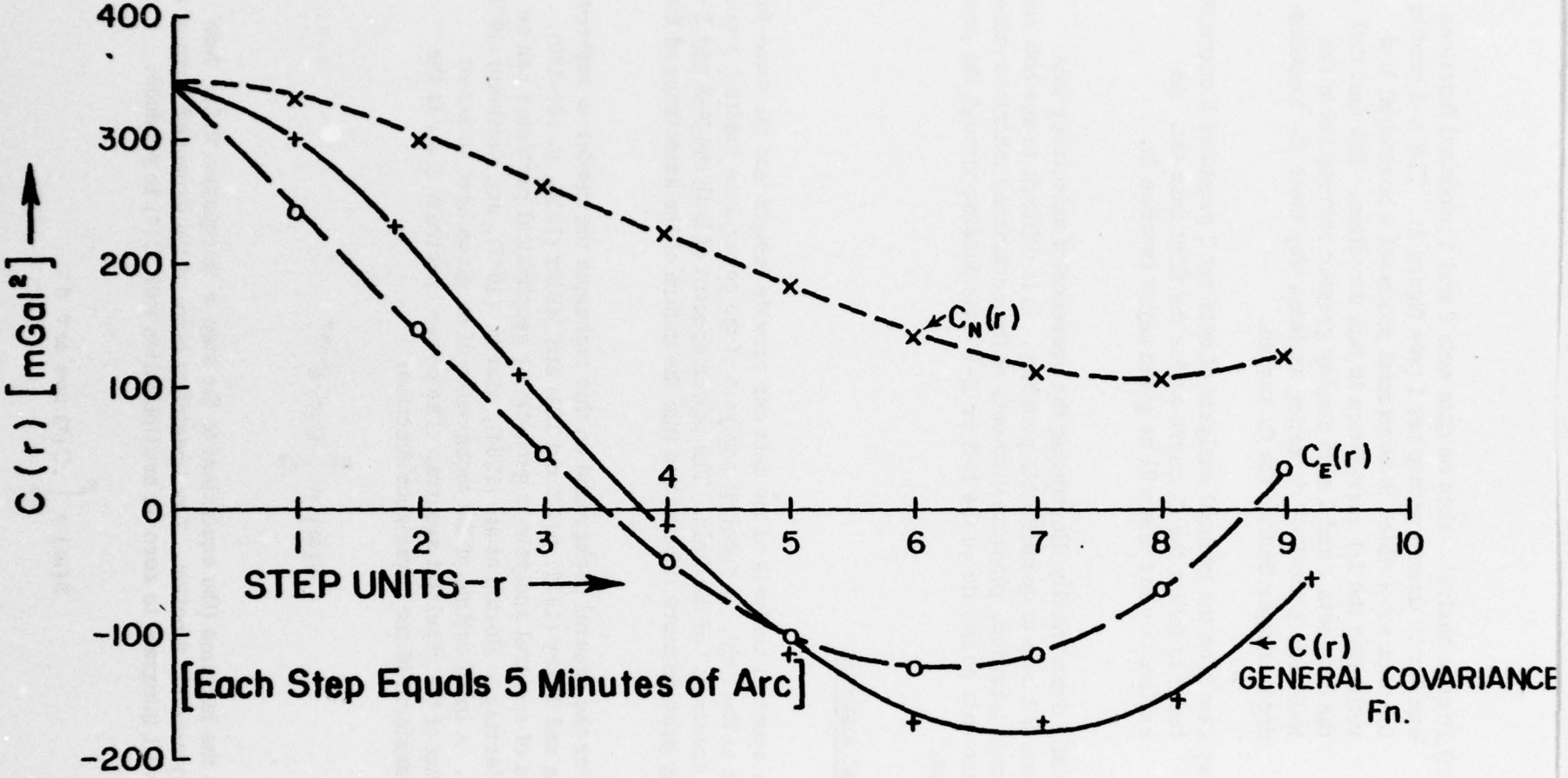

(iii) Profile analysis taken on data sets 2 and 3 produced functions similar to those for data set 1 (see figure 4). The N-S profile for data set 3 which is horizontal produced a horizontal line reflecting the 1:1 correlation in this direction. The fact that the data sets 1 and 2 also display greater correlation in the N-S than in the E-W direction explains why their C_N functions decay slower than do the C_ε curves.

(iv) One sees the general analysis of data set 2 produces a curve which tends to follow the C_ε curve as for the first data set. An explanation for this will be given below (section 3).

While dramatically illustrating the presence of anisotropy this technique does not help to quantify this property. It is difficult to see how one may, by simple adaption, generate elements of the covariance matrices (unless, of course, the data points lie on the N-S or E-W axis passing through the prediction point).

3.3 Spectral Analysis

A spectral analysis of the data can provide insight into the wave-forms contributing to the field. A spectral analysis of the covariance function produces the "power spectrum" of the field. The power spectra of both the N-S and E-W profiles may provide more information into the nature of the anisotropy of the data sets.

For the general background on this technique the reader is referred to Blackman and Tukey (1957, p. 53 and 121) and Miller (1956, p. 164-170). Applications of spectral analysis to geodetic or geophysical problems can be found by referring to Horton et al. (1964), Moritz (1967), and Nettleton (1976, p. 158-181). A brief outline of the technique will be given here to assist understanding of the resultant spectra. The power spectrum $S(\omega)$ is the Fourier Transform of the covariance function:

$$S(\omega) = \int_{-\infty}^{\infty} C(\tau)\, e^{-i\omega\tau} \qquad (3.2)$$

where τ is the lag time (the equivalent to the step r in equation 2.5). Now $C(\tau)$ is a symmetric function. The imaginary term of the expanded form of $e^{-i\omega\tau}$ ($i \sin \omega\tau$) will integrate to zero on multiplication with $C(\tau)$ to produce:

$$S(\omega) = \int_{-\infty}^{\infty} C(\tau) \cos \omega\tau \, d\tau \qquad (3.3)$$

FIGURE 4: COVARIANCE FUNCTIONS OF PROFILES

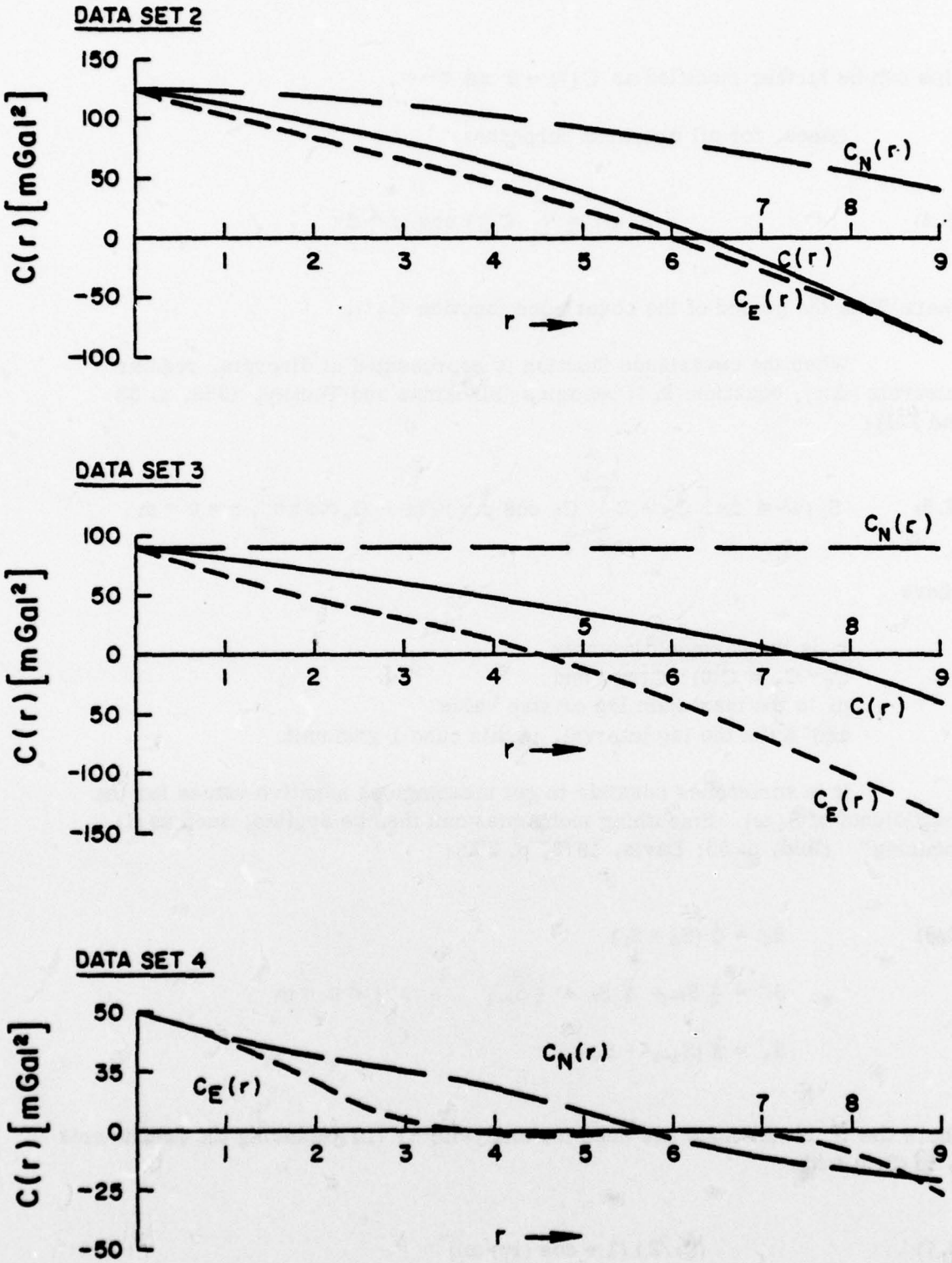

$$= 2 \int_0^{\infty} C(\tau) \cos \omega \tau \, d\tau$$

This can be further modified as $C(\tau) \rightarrow 0$ as $\tau \rightarrow \infty$.

Hence, for all practical purposes:

(3.4) $$S(\omega) = \int_0^{T} C(\tau) \cos \omega \tau \, d\tau$$

where T is the period of the covariance function $C(\tau)$.

When the covariance function is represented at discrete, regular intervals (Δx), equation (3.4) becomes (Blackman and Tuckey, 1959, p. 53 and 121):

(3.5) $$S_r(\omega) = \Delta x \left[C_0 + 2 \sum_{p=1}^{n-1} C_p \cos p \, r \, \pi/m + C_n \cos r\pi \right], \; r = 0 \rightarrow m$$

where

r is the harmonic counter
$C_0 \rightarrow C_n = C(0) \rightarrow C(m)$, and
m is the maximum lag or step value
and Δx is the lag interval, in this case 1 grid unit.

It is sometimes possible to get meaningless negative values for the coefficients of $S(\omega)$. Smoothing techniques can then be applied, such as (i) "hanning" (Ibid, p. 53; Davis, 1973, p. 269):

(3.6)
$$S_0^1 = \tfrac{1}{2} (S_0 + S_1)$$

$$S_p^1 = \tfrac{1}{4} S_{p-1} + \tfrac{1}{2} S_p + \tfrac{1}{4} S_{p+1} \qquad 1 < p < m$$

$$S_n^1 = \tfrac{1}{2} (S_{n-1} + S_n)$$

where the S^1 coefficients are used for analysis; or (ii) replacing the coefficients C_p in (3.5) with:

(3.7) $$(C_p/2) (1 + \cos (r\pi/m))$$

(see Horton et al., 1964, p. 588).

The power spectra for the N-S and E-W profiles of data sets 1, 2 and 4 are shown in Figure 5. The units of the power density estimates are mgal squared per cycle per grid unit. The abscissa is annotated in both frequency (f - cycles per grid unit) and harmonics of the fundamental wavelength (shown by arrows). See Appendix A1.

The spectra for data set 1 differ dramatically in the low order harmonics, the spectrum for the N-S profile (S_ℓ) maximizing for the zero order term while that for the E-W profile (S_N) receives its maximum contribution from the first harmonic. A similar effect is noticed in the spectra for data set 2. While this clearly shows the field is anisotropic and this is valuable information to have for (say) the removal of trend surfaces, it is not useful in the evaluation of the anisotropy of the data. In fact, these spectra must be treated cautiously because, due to the limitations placed on the covariance analysis, an incomplete wavelength of information is available for analysis.

3.4 Semi-Variograms

The semi-variogram has been used extensively in the area of interpretative geology (Matheron, 1963, p. 1250; 1965). Some mention has been made of their use for geodetic purposes (Monget, 1969; Monget and Albuisson, 1971), but their application in this field has been limited. This function is closely related to the structure function, used by Vyskočil in the statistical analysis of gravity in Czechoslovakia (Vyskočil, 1970).

The semi-variogram is defined as:

$$\gamma(r) = \frac{1}{2S} \iint_S (\Delta g_{i+r} - \Delta g_i)^2 \, dS \tag{3.8}$$

where S is the area under consideration. This function assumes statistical properties of homogeneity and isotropy and its similarity to the covariance function is noted. It is in fact related to the covariance function by the simple expression (Ibid., p. 174; Matheron, 1963, p. 1253):

$$\gamma(r) = C(0) - C(r) \tag{3.9}$$

This relationship helps in understanding the behavior of the semi-variograms for profiles of the data sets (Figure 6). These curves are the mirror images of the covariances of the profiles, originating at (0,0) on the

Figure 5: POWER DENSITY ESTIMATES FROM COVARIANCE ANALYSIS

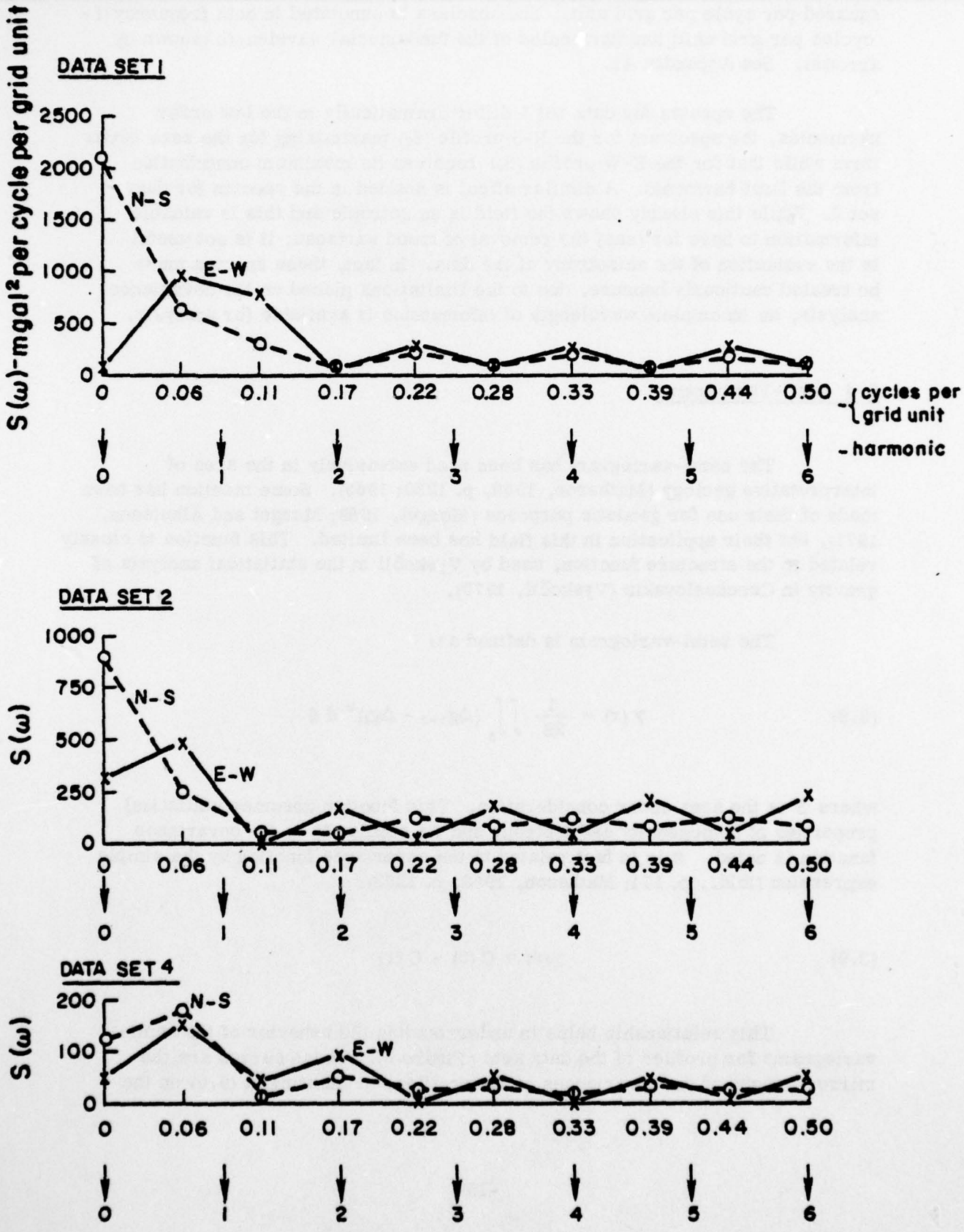

Figure 6: SEMI-VARIOGRAMS OF PROFILES

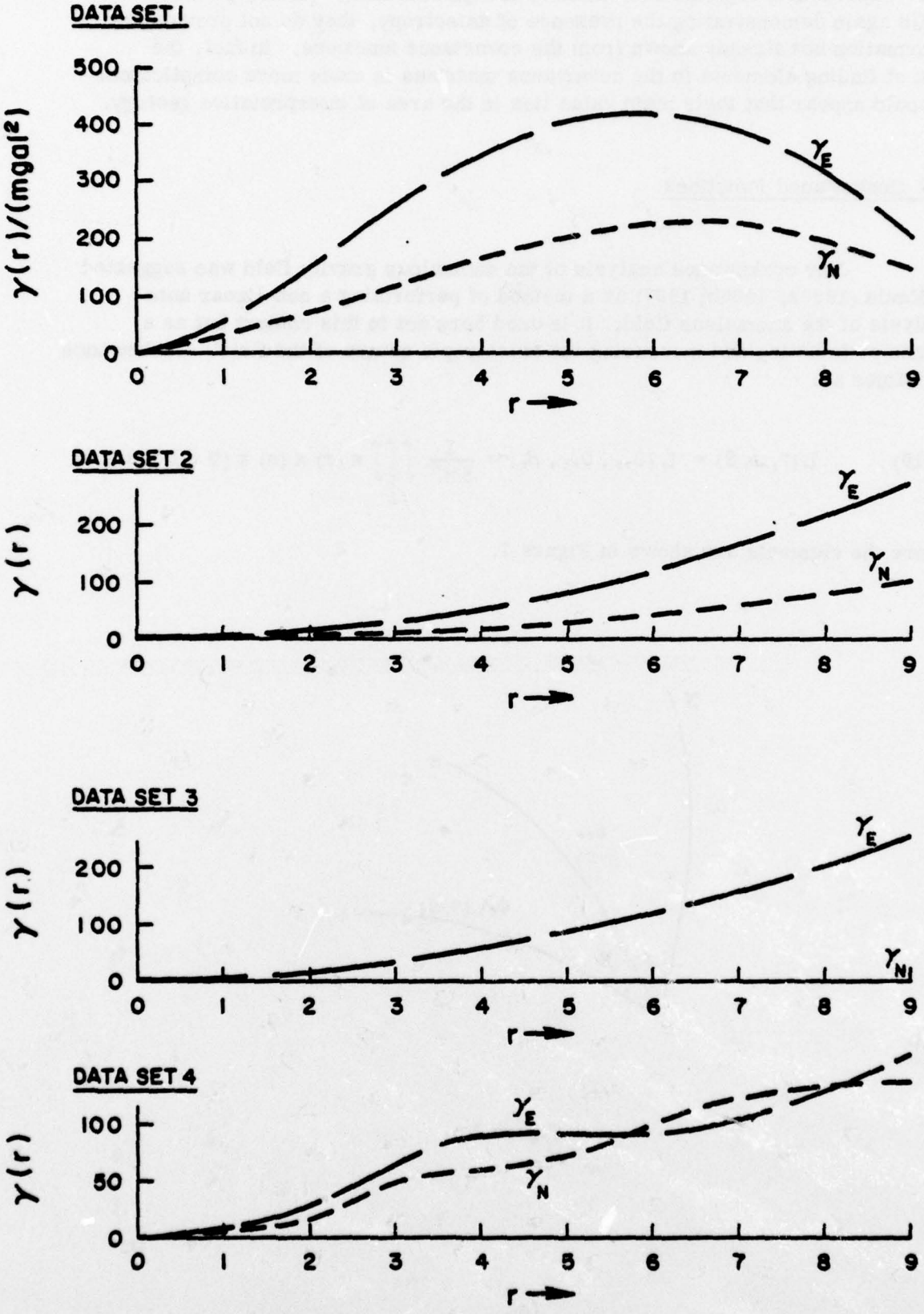

graph. According to the definitions, they fall into the "continue-type" class, i.e. "represent a regionalized variable of high continuity" (Ibid., p. 1250). While again demonstrating the presence of anisotropy, they do not provide any information not already known from the covariance functions. In fact, the task of finding elements in the covariance matrices is made more complicated. It would appear that their main value lies in the area of interpretative geology.

3.5 Coskewance Functions

The coskewance analysis of the anomalous gravity field was suggested by Kaula (1966a; 1966b; 1967) as a method of performing a non-linear auto-analysis of the anomalous field. It is used here not in this context but as a means of detecting and measuring the anisotropic nature of the field. Coskewance is defined as:

$$(3.10) \qquad L(\tau, \omega, \beta) = L(\psi_{rs}, \psi_{rt}, \beta_r) = \frac{1}{8\pi^2} \iiint x(r)\, x(s)\, x(t)\, dt\, ds\, dr$$

where the elements are shown in Figure 7.

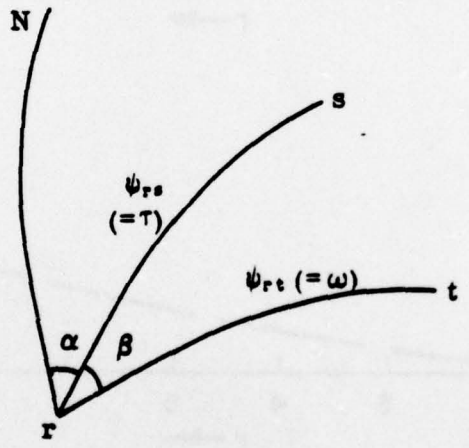

Figure 7

FIGURE 8: COSKEWANCE FUNCTIONS

(OFFSET CONFIGURATION)

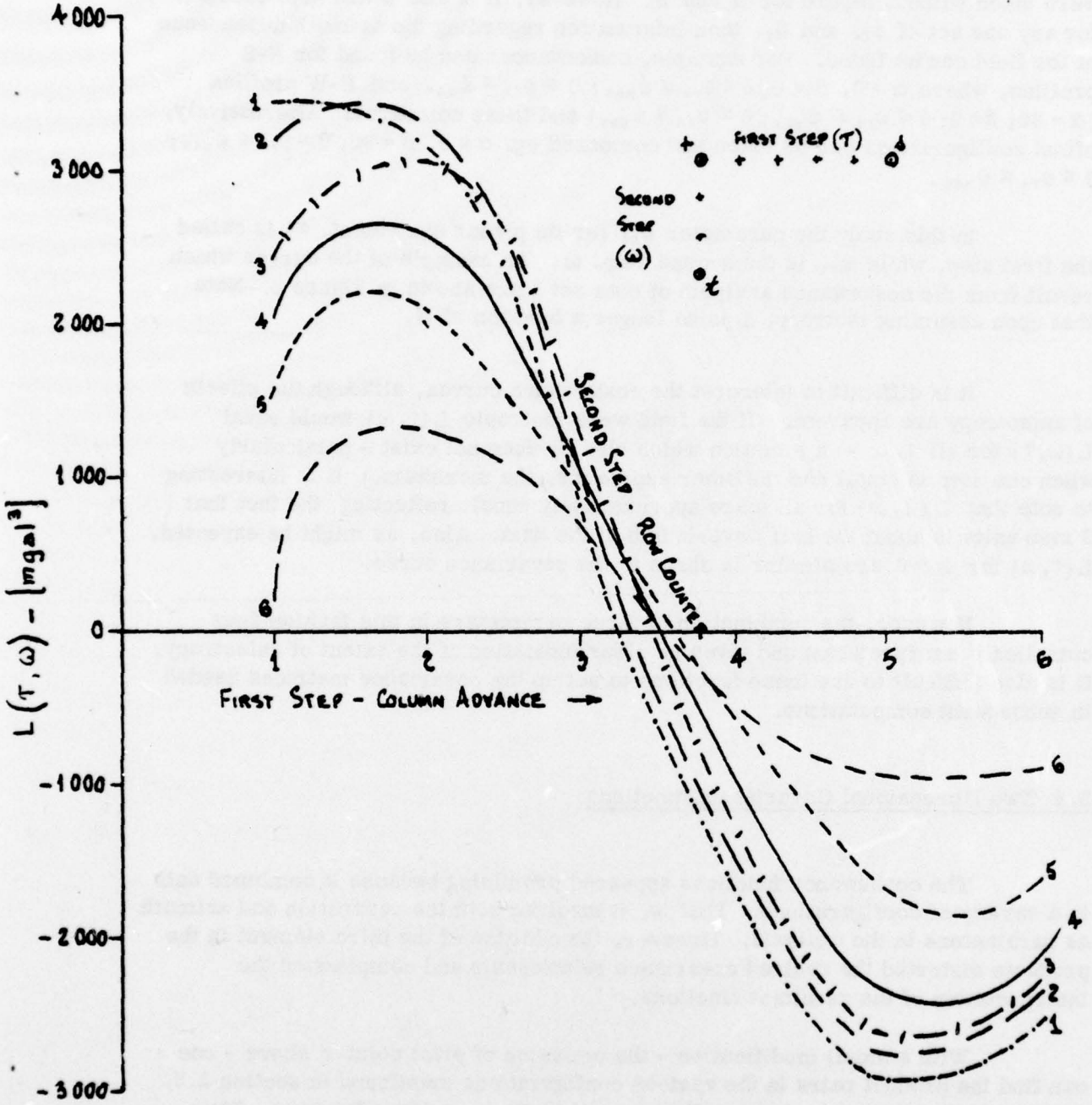

It is analogous to covariance except that triple products rather than product pairs are meaned throughout the field.

The original development assumed isotropy in the data, i.e. means were taken without regard for α and β. However, if α and β are kept constant for any one set of ψ_{rs} and ψ_{rt} then information regarding the azimuth dependence of the field can be found. For example, coskewances can be found for N-S profiles, where $\alpha = 0$, $\beta = 0$; $0 \leq \psi_{rs} \leq \psi_{max}$; $0 \leq \psi_{rt} \leq \psi_{max}$ and E-W profiles ($\alpha = 90$; $\beta = 0$; $0 \leq \psi_{rs} \leq \psi_{max}$; $0 \leq \psi_{rt} \leq \psi_{max}$) and these compared. Alternatively, offset configurations can be taken and compared eg. $\alpha = 0$, $\beta = 90$; $0 \leq \psi_{rs} \leq \psi_{max}$; $0 \leq \psi_{rt} \leq \psi_{max}$.

In this study the parameter ψ_{rs} (or its planar equivalent, τ) is called the first step, while ψ_{rt} is the second step, ω. An example of the curves which result from the coskewance analysis of data set 1 are shown in Figure 8. Note that upon assuming isotropy, L is no longer a function of β.

It is difficult to interpret the coskewance curves, although the effects of anisotropy are apparent. (If the field were isotropic $L(\tau, \omega)$ would equal $L(\omega, \tau)$ for all τ, ω - a situation which clearly does not exist - particularly when one step is small and the other approaches the maximum.) It is interesting to note that $L(3, \omega)$ for all ω are approximately equal, reflecting the fact that 3 step units is about the half wave-length of the data. Also, as might be expected, $L(\tau, \omega)$ for $\omega \to 0$ are similar in shape to the covariance curve.

However, the combination of three parameters in this fashion does complicate interpretation and gives no clear indication of the extent of anisotropy. It is also difficult to use these functions to set up the covariance matrices needed in subsequent computations.

3.6 Two Dimensional Covariance Functions

The coskewance functions appeared promising because it combined data in a variety of configurations. That is, it involved both the separation and azimuth as parameters in the analysis. However, the addition of the third element in the products distorted the desired covariance relationship and complicated the interpretation of the resultant functions.

With a small modification - the omission of pivot point r above - one can find the product pairs in the various configurations mentioned in section 3.5. The resultant function is the two-dimensional (2-D) covariance function. Thus:

$$(3.11) \qquad C(r,s) = \frac{1}{(N-|r|)(N-|s|)} \sum_{i=1}^{N-|r|} \sum_{j=1}^{N-|s|} \Delta g(i,j)\, \Delta g(i+r, j+s), \quad r, s = 0, m$$

where r, s is the step in the row, column respectively
m is the maximum step set for the analysis (usually N/2), and
N is the number of rows, columns in the array (assumed square).

This expression is algebraically correct, that is the steps in the rows and columns can be both positive and negative. It will be seen that:

and

$$C(-r,s) = C(r,-s)$$
$$C(-r,-s) = C(r,s)$$

In the resultant surface quadrants I and III are identical as are quadrants II and IV.

This function has been found useful in other areas of scientific study to depict the azimuth-dependent statistical relationships which exist between data points. For example, Whittle (1954) used it to demonstrate the auto-correlation of soil fertility as evidenced by the wheat yield of rectangular subdivisions of a test area. It has also assisted the study of magnetic anomalies in the north-western regions of Canada (Horton et al., 1964, p. 597-599). It has been used to test the anisotropic characteristics of the gravity field in the Carpathian Mountains of Czechoslovakia (Kubáčková, 1974). This area is similar in size to the test areas in this present study and data was taken at 1' x 1' intersections. The function has received mention in other gravimetric studies (e.g. Jordan, 1972, p. 3661) but this writer has found no other use of it in the geodetic literature.

The 2-D covariance analysis of data set 1 produces the surface illustrated in Figure 9. The following points should be noted:

(i) the surface represents the covariance relationships for product pairs of all separations and orientations. Note that it includes the N-S and E-W functions deduced above; these are found by taking a section through the midpoint of the figure, C(0, 0), north and east respectively.

(ii) The anisotropic character of the original data is fully quantified. The predominant direction of the isogal lines in figure 1 ($\alpha \simeq 10^{\circ}$) is reflected by the orientation of the contours of the 2-D covariance surface.

(iii) A truly isotropic data set will produce a circular pattern for the contours of the 2-D covariance surface (see Agterberg, 1970, 125; Kubáčková, 1974, 19). The extent of the deviation of the contours from circles indicates the extent of anisotropy existing in the field.

(iv) The behavior of the general covariance function (section 3.2) can now be understood. This results, of course, from the average of all profiles $0 \leq \alpha < 360$. The fact that the contours of the 2-D covariance surface run approximately N-S will mean that the average taken for any one separation (r) will tend toward the curve which is more representative of the predominant trend of the surface i.e. the C_ξ curve.

(v) Because of population differences the r.m.s. of the C (i, j) values increase with increase in i, j. For example, the spread for C (0, 0) in (the r.m.s. sense) is ± 30 $mgal^2$ while the same spread for C (+6, +6) is ± 60 $mgal^2$. This should be remembered when extracting C (i, j) values for subsequent computation.

The 2-D covariance analysis of data set 2 produces a surface with features similar to the surface just discussed (see Figure 10). However, analysis of data set 4 (adjacent to data set 1) shows that this field tends much more to the isotropic situation (see Figure 11). Insofar as it bears little resemblance to the 2-D covariance surface for data set 1, it reinforces the warning concerning the use of the covariance function derived from one local field to represent the statistical characteristics of another field, no matter how close that field may be.

3.7 Representation of the 2-D Covariance Surface

It is possible to represent the 2-D covariance surface in three ways:

(i) by surface-fitting

(ii) by a family of curves

(iii) by discrete data .

Section 4.2 shows the results of some experiments which used method (iii) to represent the 2-D covariance surface of data set 1 (Figure 9). It could be well represented by a fairly low-order surface (say of order 3, however, the approach which uses a family of curves has the distinct advantage that it directly relates to the functions already used to represent general covariances. This advantage is enhanced if one chooses a function which is compatible for covariances of all geoidal relationships (cf. Jordan, 1972).

The basic parameters which have been used to describe the normal (1-D) covariance function are:

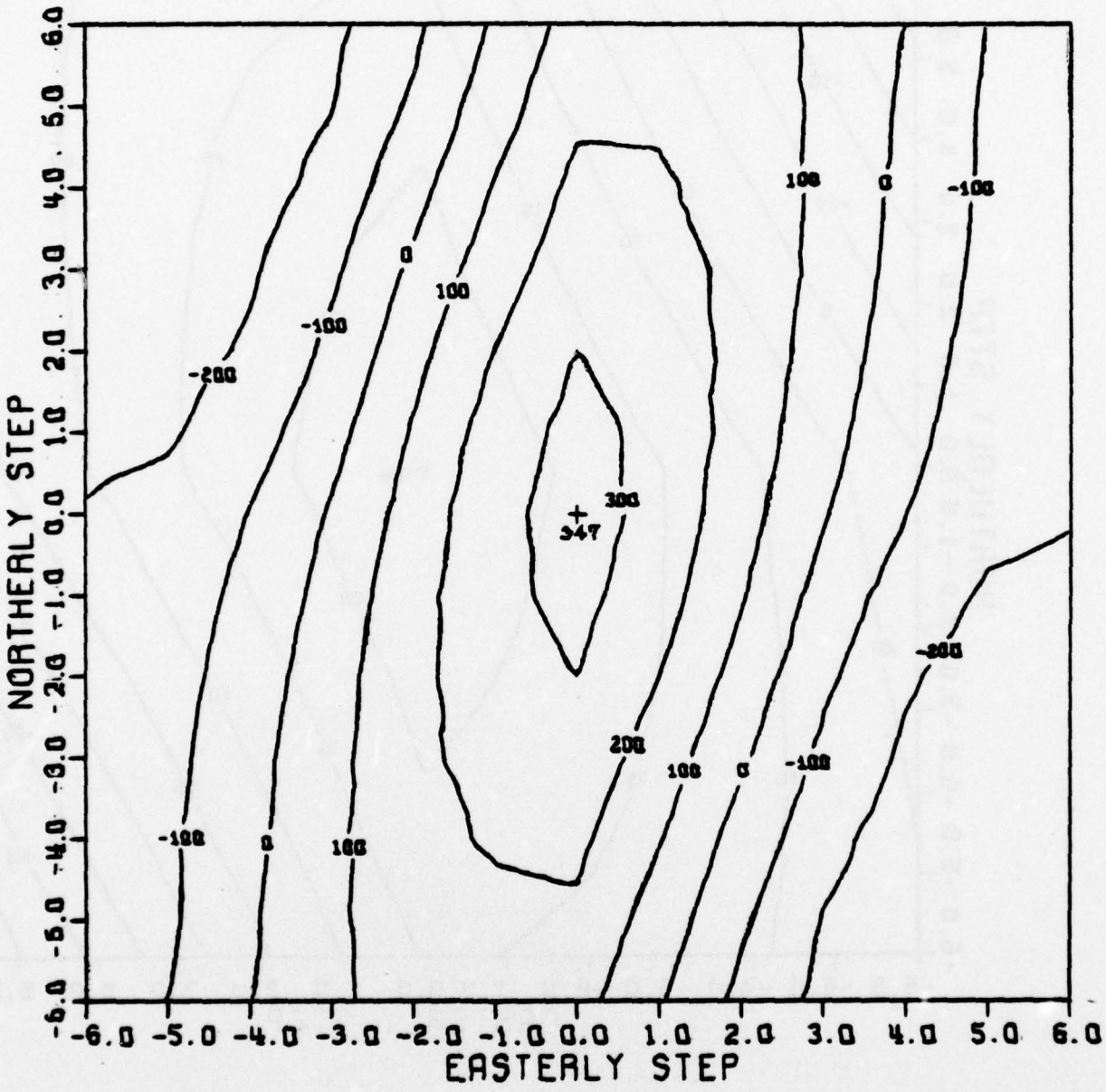

Figure 9. The 2-D Covariance Function for Data Set 1

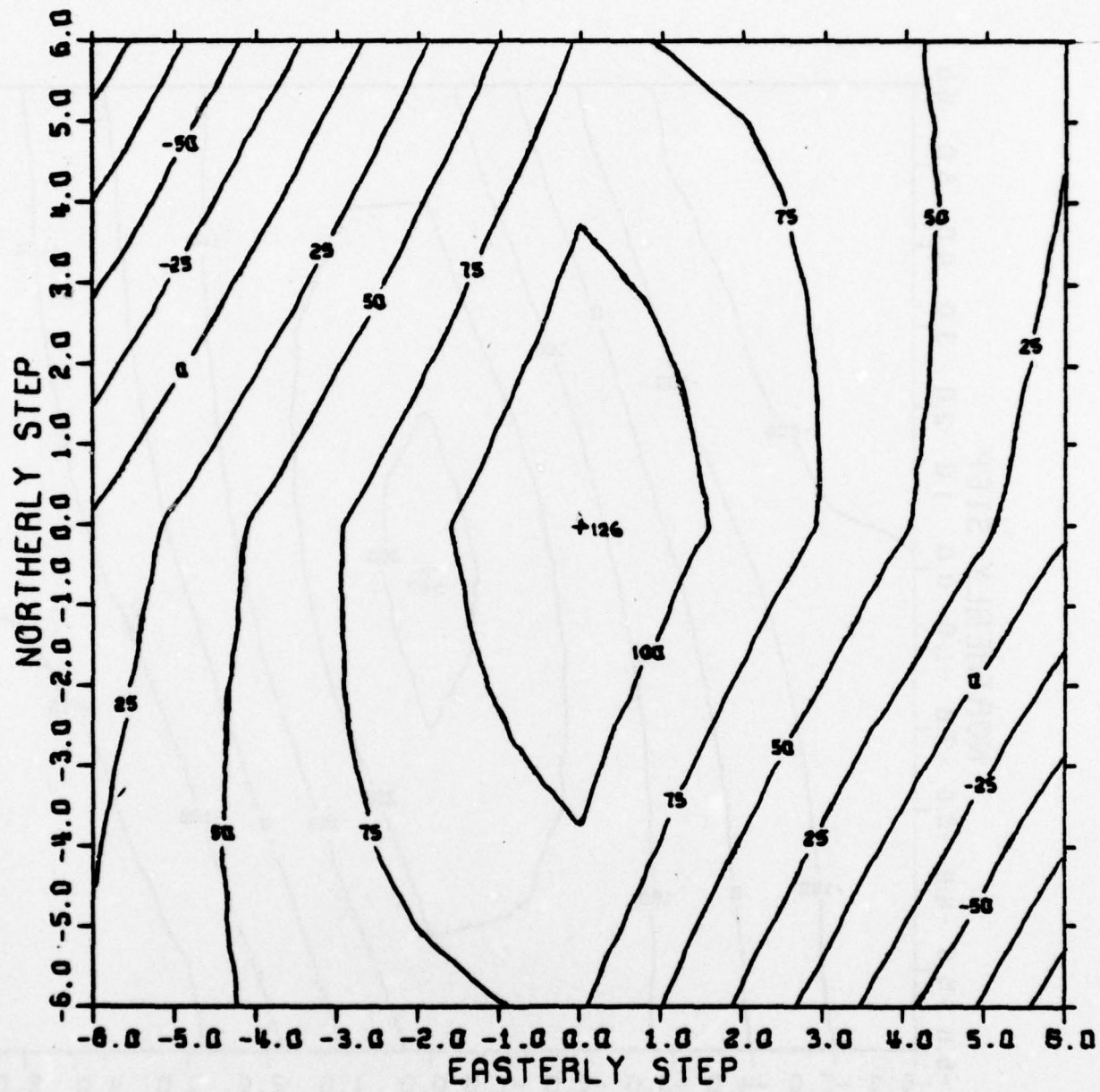

Figure 10: 2-D Covariance Function - Data Set II

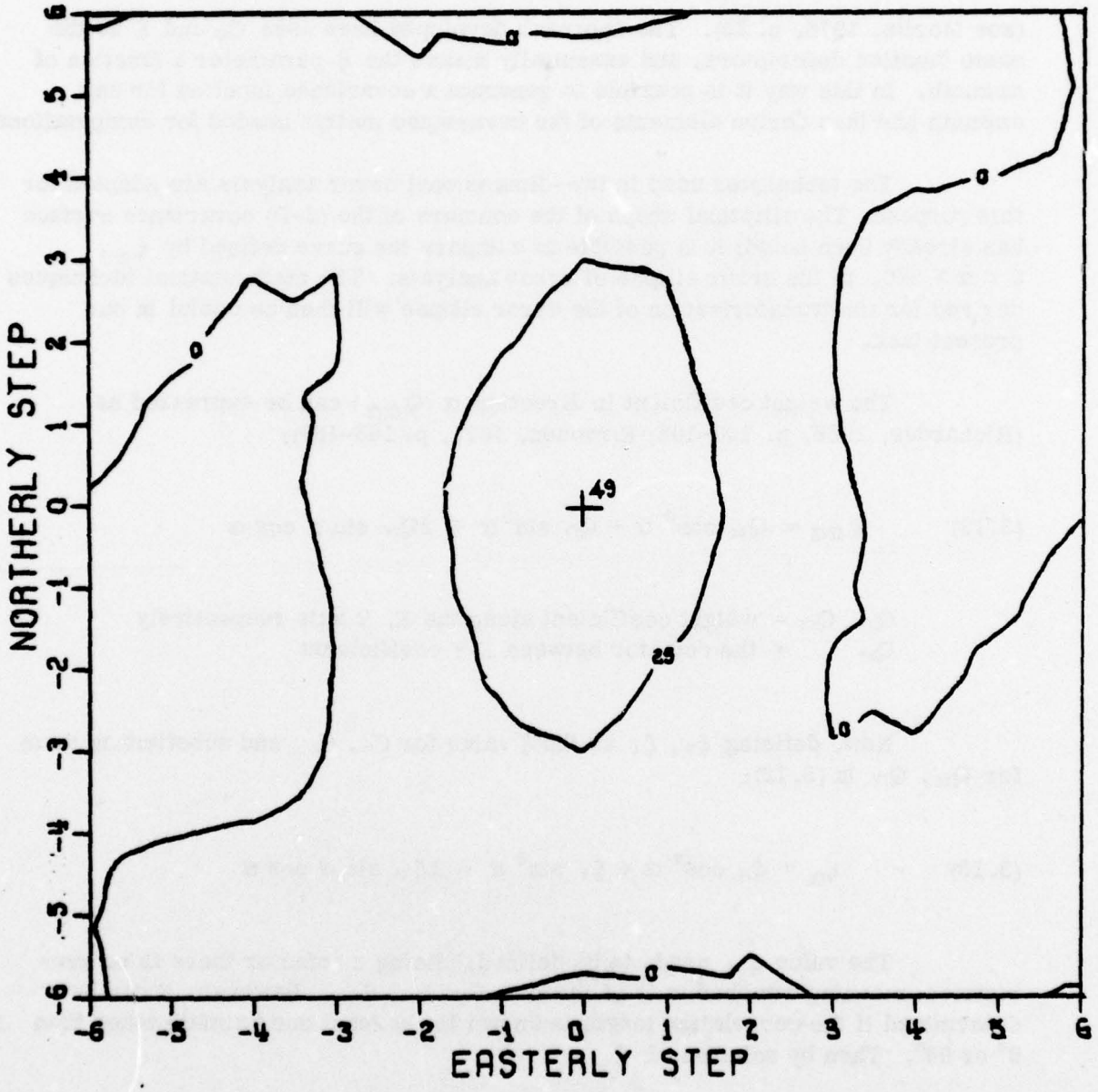

Figure 11: 2-D Covariance Function - Data Set IV

(i) C_o - the variance,

(ii) ξ - the correlation length, defined such that $C(\xi) = \frac{1}{2} C_o$, and

(iii) χ - the curvature of the curve at $r = 0$

(see Moritz, 1976, p. 22). The approach developed here uses C_o and ξ as the basic function descriptors, and essentially makes the ξ parameter a function of azimuth. In this way it is possible to generate a covariance function for any azimuth and thus derive elements of the covariance matrix needed for computations.

The techniques used in two-dimensional error analysis are adapted for this purpose. The elliptical shape of the contours of the (2-D) covariance surface has already been noted; it is possible to compare the curve defined by ξ_α, $0 < \alpha \leq 360$, to the error ellipse of error analysis. The mathematical techniques derived for the transformation of the error ellipse will then be useful in our present task.

The weight coefficient in direction α ($Q_{\alpha\alpha}$) can be expressed as (Richardus, 1966, p. 100-105; Hirvonen, 1971, p. 165-169):

$$Q_{\alpha\alpha} = Q_{xx} \cos^2 \alpha + Q_{yy} \sin^2 \alpha + 2Q_{xy} \sin \alpha \cos \alpha \tag{3.12}$$

Q_{xx}, Q_{yy} = weight coefficient along the X, Y axis respectively
Q_{xy} = the cofactor between X Y coefficients

Now, defining ξ_N, ξ_E as the ξ value for C_N, C_E, and substituting them for Q_{xx}, Q_{yy} in (3.12):

$$\xi_\alpha = \xi_N \cos^2 \alpha + \xi_E \sin^2 \alpha + 2\xi_{NE} \sin \alpha \cos \alpha \tag{3.13}$$

The value ξ_{NE} needs to be defined. Being a cofactor there is no geometrical meaning attached to it as there is for ξ_N, ξ_E. However, it can be determined if the correlation length is known for at least one azimuth other than 0° or 90°. Then by solution of:

$$\xi_{NE} = [\xi_{\alpha\alpha} - (\xi_N \cos^2 \alpha + \xi_E \sin^2 \alpha)] / 2 \sin \alpha \cos \alpha \tag{3.14}$$

this quantity can be determined. The most sensitive estimate would be obtained for a mid-quadrant azimuth, and to control the discrepancies occurring due to the departure of the ξ curve from a true ellipse, two values of ξ_{NE} were obtained from $\alpha = 45°$ and $\alpha = 135°$. The mean of these was then substituted into (3.13). This expression could then be used to generate the covariance function for any azimuth.

Local Covariance Functions

Many expressions have been suggested to represent the local covariance function. Experiments were made on a selection of these to determine which was best suited for surface generation. Those tested are listed below. The parameter s represents the step or lag throughout.

Model 1: Hirvonen's covariance function (Hirvonen, 1962; Moritz, 1976, p. 17)

(3.15) $$C(s) = C_o / \left\{1 + (s/d)^2\right\}$$

For this function $\xi = d$

Model 2: The Gaussian function (Ibid., p. 18, 26)

(3.16) $$C(s) = C_o \, e^{-A^2 s^2}$$

For which $\xi = \frac{1}{A} (\ell n \, 2)^{\frac{1}{2}}$

Models 3 and 4:

These were Models 1 and 2 compounded with the cos term, $\cos(r\pi/\lambda)$. This was done in order to obtain the characteristic negative values for the covariance function. Unmodified, Models 1 and 2 approach zero, but never become negative. The wavelength (λ) of 6 units as used in the spectral analysis was again adopted. However, difficulty was encountered in maintaining the ξ values for this wavelength, and the results obtained were generally poor. They are omitted from the summarized results in Table 2.

Model 5: The logarithmic model (Moritz, 1976, p. 29)

$$C(s) = \frac{C_0}{A} \ln \frac{2e^A}{1+(1+k^2s^2)^{\frac{1}{2}}} \quad , \tag{3.17}$$

$$\text{where } \xi = k^{-1}\left\{(2e^{A/2}-1)^2 - 1\right\}^{\frac{1}{2}}$$

Assuming $k = 1$ to maintain the accepted values for the curvature parameter (Ibid.).

$$A = 2 \ln \left[\frac{1+(\xi^2+1)^{\frac{1}{2}}}{2}\right]$$

Model 6: The third-order Markov model (Jordan, 1972, p. 3664)

$$C(s) = C_0 \left(1 + \frac{s}{D} - \frac{s^2}{2D^2}\right) e^{-s/D} \tag{3.18}$$

ξ is found to be approximately 1.095 D (Ibid., p. 3665). This function is of interest because of its compatibility with the auto- and cross-correlation functions of other derivatives of the anomalous potential.

Using all models, C(s) was found for all s, $1 \le s \le 5$, with ξ_α computed from (3.13) for azimuths $0 \le \alpha < 360$ in 10° advances. A selection of these are tabulated in Table 2, and compared with the actual discrete values of the 2-D covariance. Also, out of interest, the values for the general covariance function are listed.

The comparisons indicate that the logarithmic model (model 5) appears to give the best all around results. All models fit well for $\alpha = 0$ where the curve attenuates slowly. The poorest fit is found for negative covariances, and it is in this region that model 5 is clearly superior. It must be noted that discrepancies in azimuths 50° and 130° will be influenced by the approximation of the ξ-generator (equation 3.13) to the actual ξ curve. These discrepancies could be minimized by the adoption of a more sophisticated expression to determine ξ_α.

It appears that this technique is quite successful. It must be pointed out that generation of covariances in this way comes much closer to the truth than the values found from the general covariance function based on an isotropic statistical model. Whether or not this improvement in accuracy is significant must be the subject of a further investigation (section 4.1).

Table 2

Generated Covariances
($mgal^2$)

Azimuth	Step	Model					
		2-D	General	1	2	5	6
0°	1	332	300	334	337	318	318
	2	300	208	299	310	272	274
	3	263	88	255	270	233	235
	4	223	- 13	211	223	200	203
	5	180	-110	173	173	173	177
50°	1	275	300	286.	299	285	284
	2	175	208	187	192	188	186
	3	50	88	118	92	106	101
	4	-100	- 13	79	33	37	31
	5	-200	-110	55	9	- 20	- 27
90°	1	270	300	261	276	267	268
	2	143	208	150	140	143	145
	3	8	88	88	45	37	40
	4	- 99	- 13	56	9	- 50	- 47
	5	-170	-110	37	1	-124	-120
130°	1	300	300	327	332	312	313
	2	245	208	278	292	259	261
	3	175	88	222	235	212	217
	4	100	- 13	175	175	174	180
	5	20	-110	136	118	142	149

3.8 Conclusions

The 2-D covariance function promises to be the most efficient way of detecting and representing anisotropy in a local or regional data set. It clearly illustrates the extent to which the data departs from an isotropic situation. Because it represents the covariance relationships which exist between point pairs of all separations and orientations, it is easily used to generate elements in the covariance matrices for prediction or collocation computations.

The 2-D covariance surface can be represented by means of a family of curves, generated using C_o computed in the analysis, and the correlation length ξ found for four azimuths from the covariance surface. The logarithmic model of Moritz (model 5) appears to represent the surface most successfully. It is thought that an improvement in the ξ generator would similarly improve the covariance values in the mid-quadrant directions.

4. The 2-D Covariance Function in Collocation and Prediction

4.1 Introduction

The 2-D covariance function represents the covariance relationships of point pairs of all separations and orientations. The question now arises as to the possibility of using this function in collocation and prediction computations. Most theoretical developments which derive analytical expressions to account for an anisotropic situation modify these by assuming isotropy before continuing with the investigation (e.g. Jordan, 1972, p. 3663; Grafarend and Offermans, 1975, p. 14). This occurs even for the cross-covariances of the deflections of the vertical. These are shown to be azimuth dependent whether or not the potential field is assumed isotropic (Moritz, 1972, p. 111; Grafarend and Offermans, 1975, p. 14). However, it should be noted that if the potential field is assumed isotropic, the expressions for the above cross-covariances are, in fact, a modification of the more complete expressions which account for anisotropy (Ibid., p. 15).

However, there appears to be no theoretical objection to the use of the 2-D covariance function in collocation or prediction solutions. The computation is thought to be in a planar rather than a linear (or time) domain. The contribution of the known element to the unknown is now dependent on its directional, as well as its 'temporal', position on the plane. The a_{pi} in equation (2.14) accounts for this, for the elements of the array C_{pi} are now derived having regard to the relative position of the signal point vis-a-vis the known point. Similarly, the C_{ij} matrix is developed by noting the disposition of each data point to all other data points in turn. These values can be generated using techniques described in section 3.8. However, in the experiments below, values have been taken directly from the arrays resulting from the 2-D covariance analysis.

4.2 Results of Prediction Tests

The aim of the tests was to compare results of predictions made using the 2-D covariance function with those resulting from use of the general covariance function. Data sets 1 and 2 were used in these tests as these were two fields exhibiting strong azimuth dependent characteristics.

In the test eight "known" points were used to estimate an unknown point. (This number if close to the optimum suggested by Rapp (1964, p. 141) for the prediction of point anomalies.) These eight points were chosen in various configurations in order to exaggerate the effect of the anisotropy of the field (see Figure 12). This configuration was "stepped" through the data array, and the differences between true and predicted values used to find the actual r.m.s. error of prediction. This value was also compared with the theoretical r.m.s. error derived from equation (2.16). See Table 3 for definitions.

4.2.1 Configuration 1

(i) Data Set 1

The results of prediction using the 2-D covariance function are marginally worse than those using the general function (see Table 3). The distribution of errors is similar (see Figure 12), although an inspection of a plot of these differences shows that the 2-D function consistently produces larger discrepancies. It appears that the data points closest to P (the prediction point) have the greatest influence on the predicted value. Their proximity to P (1.4 step units) meant that there was no significant difference between the 'weights' produced from the 2-D and the general covariance functions. For example, $C_{P_1}(1.4) = 260$ mgal^2 of $C_{P_1}(1,1) = 245$ mgal^2 and $C_{P_1}(1,-1) = 240$ mgal^2. It could be argued that a lack of homogeneity throughout the field meant that the 2-D covariance function was unrepresentative of the average situation throughout the whole data set, and it was adequate to assume a fully random statistical relationship between point pairs at this small separation.

(ii) Data Set 2

In this case the effect of anisotropy is felt. The 2-D function produces an r.m.s. of ± 11.6 mgal (and $m_p = \pm 7.1$ mgal) while the general function gives rise to an r.m.s. of ± 13.4 mgal (and an m_p of ± 11.7 mgal). This is not unexpected in this extreme case. The fact that the difference is not larger must in part be due to the proximity of the closest points to P. (See also the distribution of differences, Figure 12).

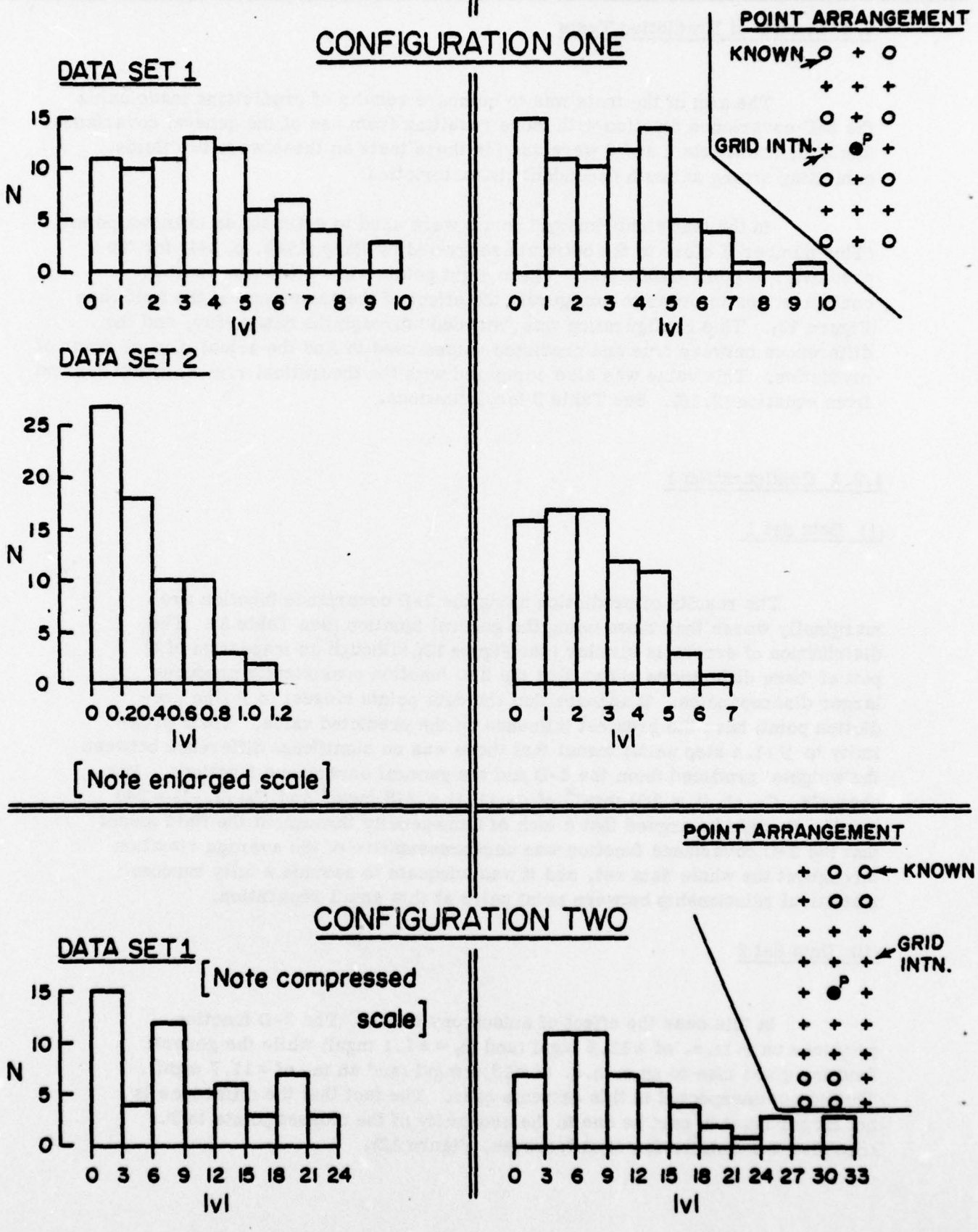

FIGURE 12 : RESULTS OF PREDICTION TESTS [Units: mgal]

4.2.2 Configuration 2

(i) Data Set 1

Configuration 2 was deliberately chosen to maximize the difference between the general function and the 2-D function. For example, C (3,1) = 240 $mgal^2$ and C (4,0) = 220 $mgal^2$ while the general function equivalents, C (3.2), C (4), were 70 $mgal^2$ and -12 $mgal^2$ respectively. Results of the tests showed that the anisotropic model fitted the data better (m_p = ± 7 mgal for the 2-D model and ± 12 mgal for the isotropic model). A similar improvement existed in the actual error of prediction (±14 mgal cf. ±16.5 mgal). This supports the contention that the choice of an isotropic model does not always produce the optimal solution. It also underlines the danger of using the parameter m_p without reservation as an estimate of the error of prediction.

(ii) Data Set 2

The 2-D covariance function produces a very low 'actual' error (± 0.6 mgal), m_p being computed at ±4 mgal. However the solution using a general covariance function breaks down. Individual errors of up to 100 mgal are produced and the value for m_p shows a large error of prediction. Apparently, it is not possible to perform any meaningful prediction (with an asymmetric configuration) using the general function, when conditions such as those in data set 2 exist.

Table 3

Statistical Analysis of Prediction Tests

	Configuration 1				Configuration 2			
Covariance Function	Data Set 1		Data Set 2		Data Set 1		Data Set 2	
	2-D	General	2-D	General	2-D	General	2-D	General
r.m.s.(*) ± (mgal)	4.4	4.0	11.6	13.4	14.0	16.5	0.6	7.1(?)
m_p (+) ± (mgal)	7.1	6.2	4.6	5.8	7.1	11.7	4.0	11.3(?)
$\sum_i a_{p_i}$	1.16	1.16	1.05	0.68	1.07	1.09	1.04	-5.48

(*) - $[\sum (\text{predicted } \Delta g - \text{actual } \Delta g)^2 / \text{no. of predictions}]^{\frac{1}{2}}$

(+) - error of prediction - see equation (2.16)

Attention is now directed toward the third row of Table 3 where the sums of the coefficients:

$$a_{p_i} = C_{p_i}^T \bar{C}_{ij}^{-1}$$

(derived from equation 2.14) are listed. These coefficients are basic in the evaluation of both the predicted value of Δg (equation 2.8) and the theoretical estimate of accuracy (equation 2.16). It is of interest to note therefore, that in general, the most accurate results were obtained from that covariance function giving the $\sum_i a_{p_i}$ closest to unity.

It is difficult to know the actual significance of this. Equation 2.8 looks similar to the normal "weighted mean" in this context, but is not identical to it. It has already been noticed that $\sum a_{p_i}$ is not necessarily unity (Rapp, 1964, p. 7). In some cases it is valid to adjust the individual elements of the a_{p_i} vector to let the sum equal unity. In this regard it is worth quoting from Holloway (1958, p. 354-355) "The sum of the weights of a smoothing or filtering function determines the ratio of the mean of the smoothed or filtered series to the mean of the original series. In smoothing it is generally desired to leave the mean of the series unchanged, so $\sum a_{p_i}$ made equal to unity. With some filters it is not necessary to preserve the mean of the series and in these cases, $\sum_i a_{p_i} \neq 1$."

In the prediction context it is desirable that the property of ergodicity hold. It therefore appears that the covariance function which produces the $\sum_i a_i$ nearest unity is the one which maintains this property best; hence it produces the best comparisons of predicted values versus known. On the other hand, computations with $\sum_i a_i$ made equal to unity showed that some caution must be observed when modifying the coefficients in this fashion. This was particularly the case when the $\sum_i a_{p_i}$ differed greatly from unity (e.g. 0.50). In this case, although the m_p value improved, some predictions changed markedly ($\simeq$ 30 mgal) and the calculated r.m.s. deteriorated. (See starred items, Table 4, Section 4.3.) However, when the difference between $\sum_i a_{p_i}$ and unity was small and such modifications made, a slight improvement in prediction was noticed (again see Table 4).

4.3 Results of Collocation Tests

4.3.1 Introductory Remarks

The area chosen for the tests was the region near the SE coast of the United States used for calibration of Geos-3. It is bounded by $40 \geq \varphi > 20$ and $297 \geq \lambda \geq 277$, the information on latitude 20° being deleted because the larger anomaly values here introduced erratic behaviour into the covariance functions. The gravity data was in the form of 1° x 1° mean free-air anomalies extracted from the file of world-wide 1° means held at the Department of Geodetic Science. The separations (N) have been computed in this area using the GEM 6 potential coefficients to degree 16 and 1° x 1° gravity data (Rapp and Rummel, 1975). Representations of these data sets are illustrated in Figures 13 and 13a, respectively.

The aim of the collocation test was to compute the geoidal separation (N) from the gravity anomalies. The computation can be thought of as a "multivariate" prediction as defined by Grafarend (1976, p. 152) because the model effects are already assumed to be removed. (In other words the parameters AX in equation 2.19 have been computed independently and the effects of normal gravity removed from the observed gravity to obtain the free-air anomalies.)

The computations must be considered preliminary, although the author considers them to be a good approximation to a more rigorous solution. The reasons for this are as follows:

(i) Sphericity of the earth (i.e. the convergence of the meridians) was not accounted for and the data was assumed planar. Computations of the general covariance and profile covariance functions assuming a spherical model showed no appreciable change from the same functions derived using a plane model. Any difference was certainly minor when compared with the difference found between the general covariance functions and the 2-D functions.

(ii) The mean anomalies were treated as if they were point anomalies in the analysis process, as described by Smith (1974, p. 33). All auto and cross-covariances were computed from the known data. That is, no attempt was made to represent the covariances from previously determined models.

(iii) It should be remembered that this test is to obtain a comparison of the 2-D function against the 1-D function. Any shortcomings due to the approximations mentioned above will affect both equally. The validity of the comparison will therefore not be harmed to any significant degree.

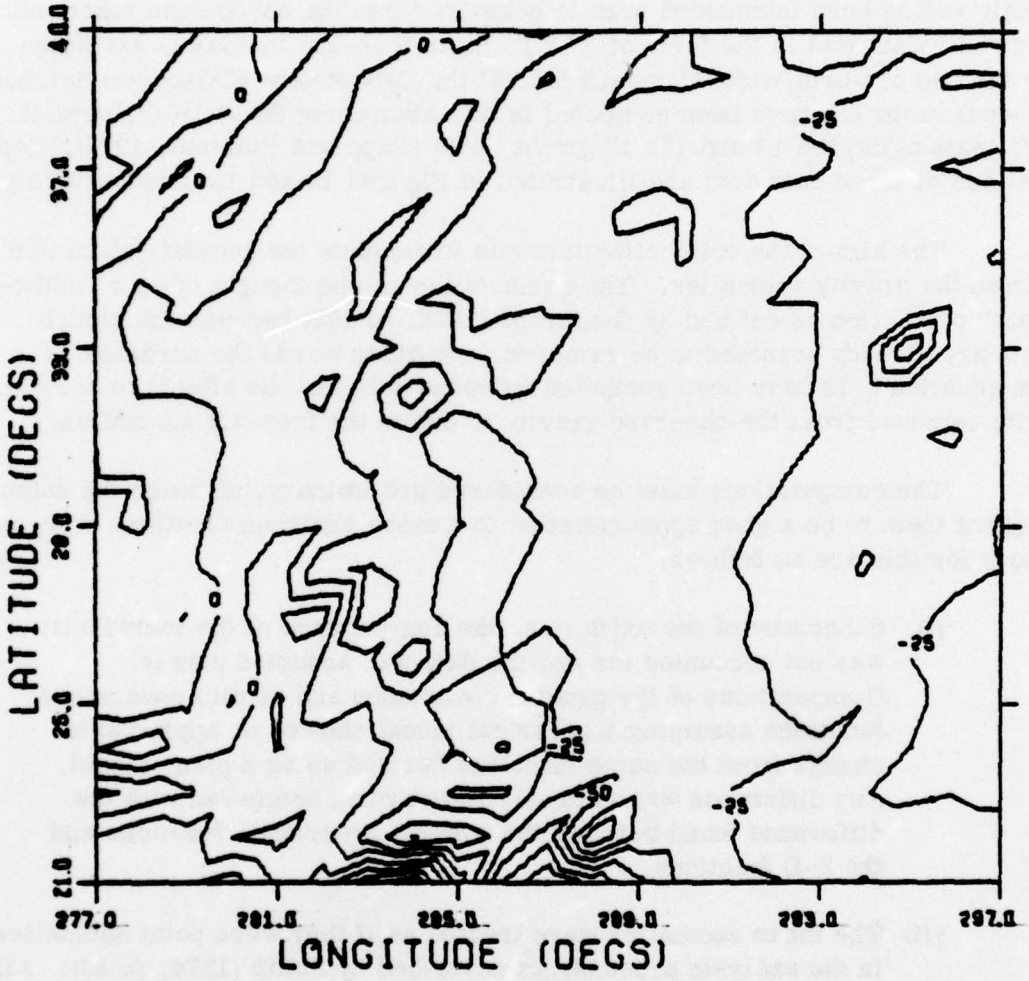

Figure 13: Free-air Anomalies - U.S. Calibration Area (Contour Interval: 25 mgal)

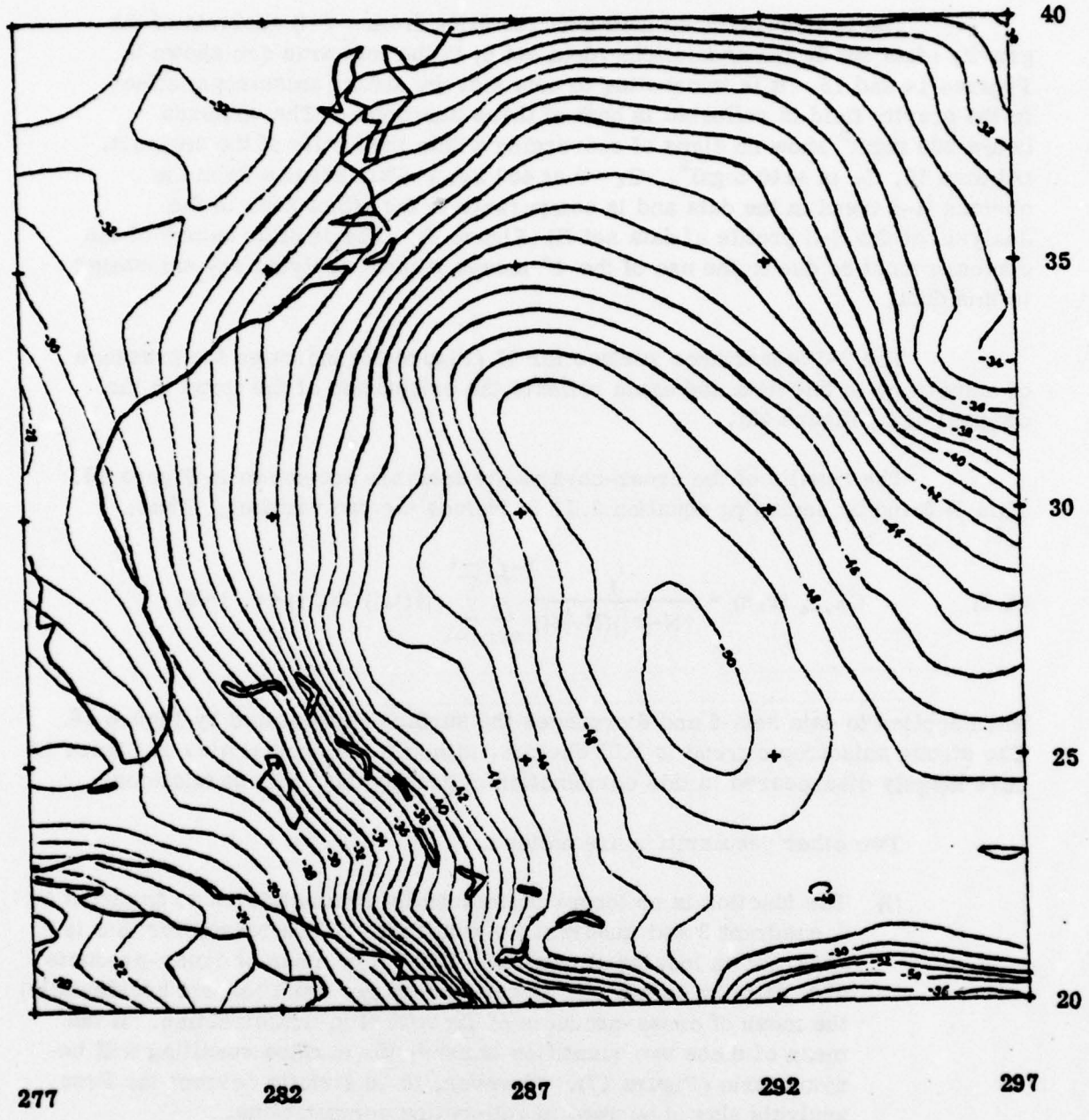

Figure 13a. Geoid Undulation Using Method B with GEM 6 Coefficients Truncated at Degree 16 and with a Cap Size of 20°. (See Rapp and Rummel, 1975, p. 18)

4.3.2 Auto and Cross-Covariance Analysis

The auto-covariance functions resulting from a 2-D analysis of the gravity (data set 5) and undulations (data set 6) in the test area are shown in Figures 14 and 15. (It is interesting to note that the strong anisotropic effect in the gravity field is reflected in both of these functions.) The contours below 200 $mgal^2$ show no signs of converging within the limits of the analysis. (At step 10, C_N is +140 $mgal^2$. $C_t = 0$ at 450 km.) This results from the obvious N-S trend in the data and is comparable to the effect seen in the analysis of the N-S profile of data set III (Figure 4). The angular nature of the contours must be due to the use of the 1° means without applying any smoothing to this data.

The 2-D covariance surface for N (Figure 15) indicates the presence of anisotropy in this data and again reflects the orientation of the trend in the original data (Figure 13).

The results of the cross-covariance analysis are shown in Figure 16. This is found by amending equation 3.11 to include the two variates. Thus:

$$(4.1) \qquad C_{N,\Delta g}(r,s) = \frac{1}{(N-|r|)(N-|s|)} \sum_{i=1}^{N-r} \sum_{j=1}^{N-s} N(i,j)\ \Delta g\,(i+r,\ j+s)$$

when applied to data sets 5 and 6 produces the surface represented by Figure 16. The strong anisotropic trend is still obvious, although the angularities of Figure 14 have largely disappeared in this combination of gravity data with undulations.

Two other pecularities are noticed.

(i) The function is no longer diametrically symmetric, i.e. quadrant 1 ≠ quadrant 3 and quadrant 2 ≠ quadrant 4. The reason for this is apparent on looking at equation (4.1). The mean of cross-products of N with Δg in any one direction does not equal (except accidentally) the mean of cross-products of Δg with N in that direction. If the mean of these two quantities is used, the surface resulting will be symmetric (Figure 17). However, to be strictly correct the first analysis should be used in collocation computations.

(ii) The function does not necessarily behave in the same way as the auto-covariance function insofar as C(0,0) is not necessarily the maximum value achieved by the surface. For example, whereas C(0,0) = 101.4 ± 9.8, C(1,0) = 106.1 ± 9.5; C(0,1) = 103.4 ± 9.2 and C(-2,1) = 104.2 ± 9.0. The author has seen no mention of this phenomenon in the literature and it is something which should be recognized as a possible characteristic of the cross-covariance analysis. However, because the increase from C(0,0) is small

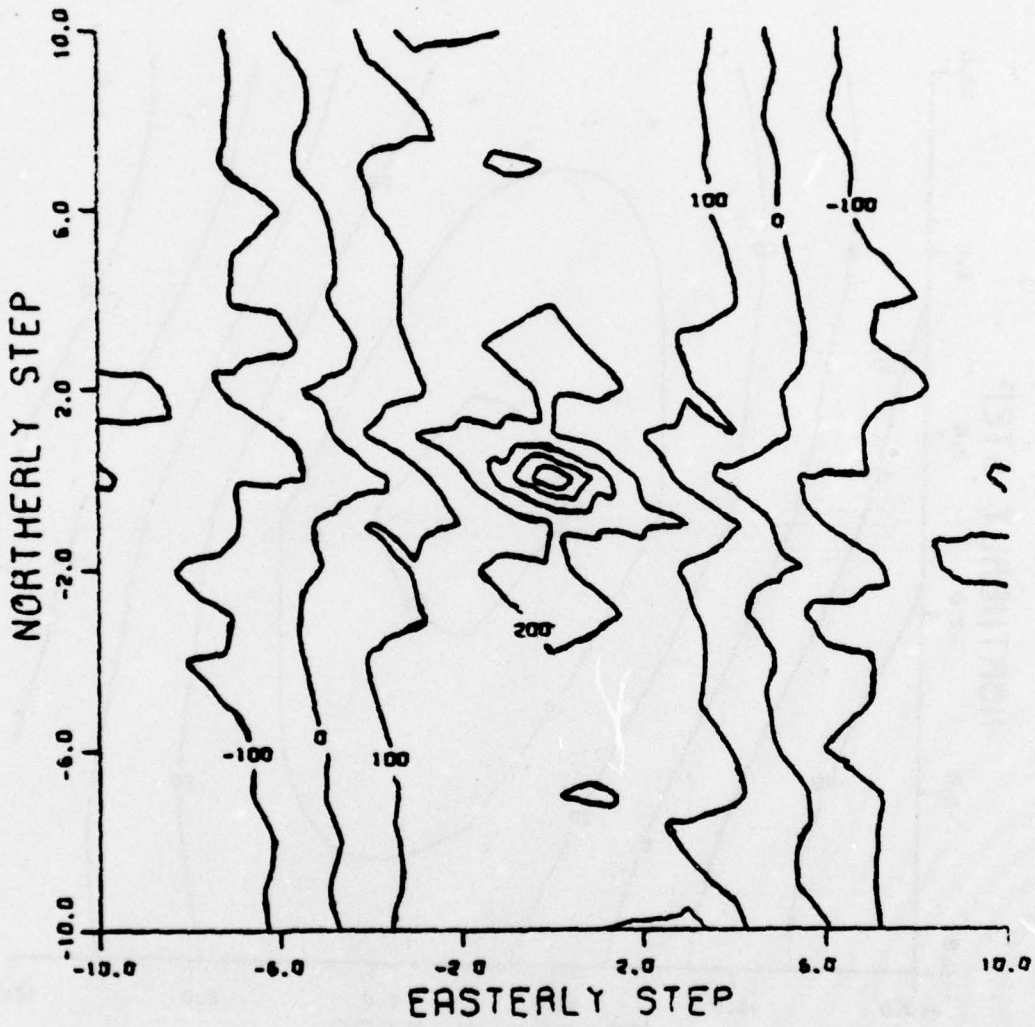

Figure 14: 2-D Auto-covariance Function - Data Set 5
(Contour Interval: 100 mgal^2)

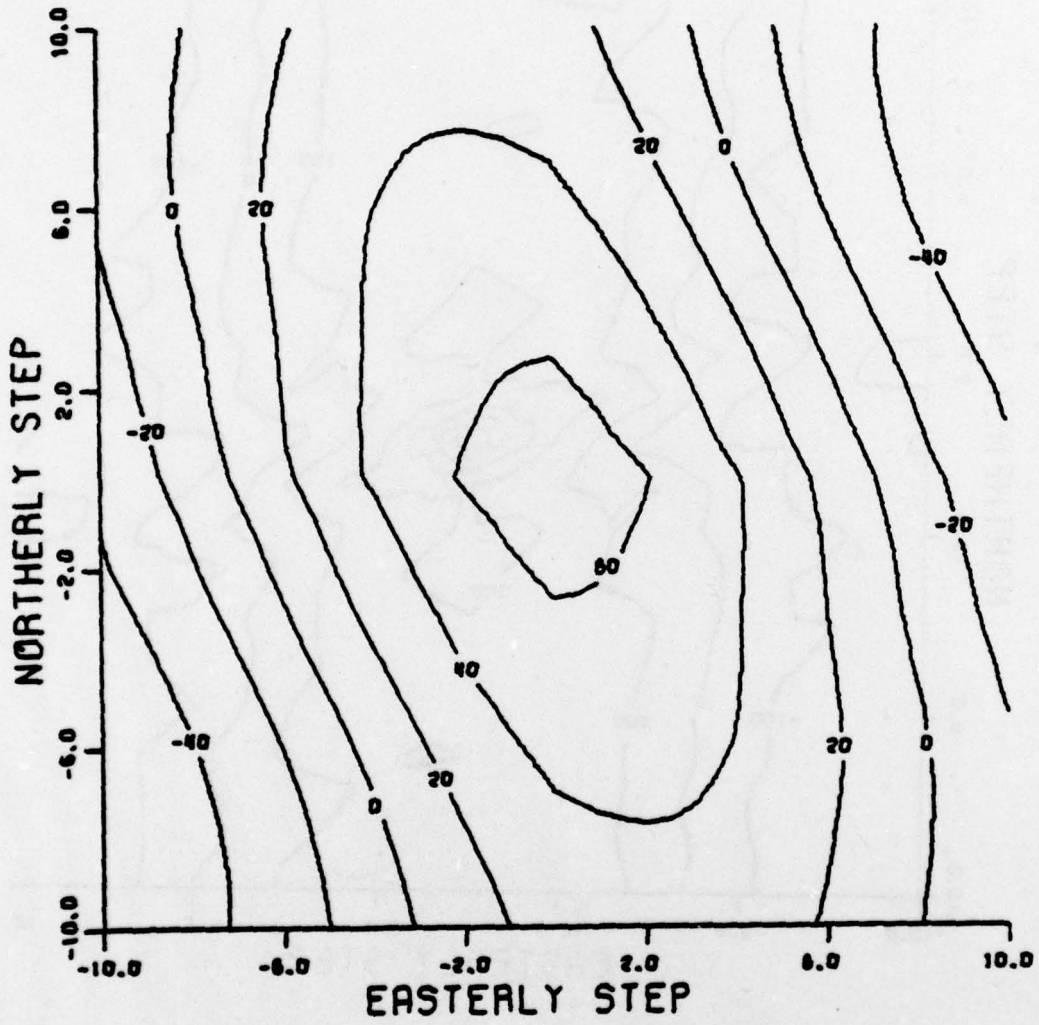

Figure 15: 2-D Auto-covariance Function for N
(Contour Interval: $20 m^2$)

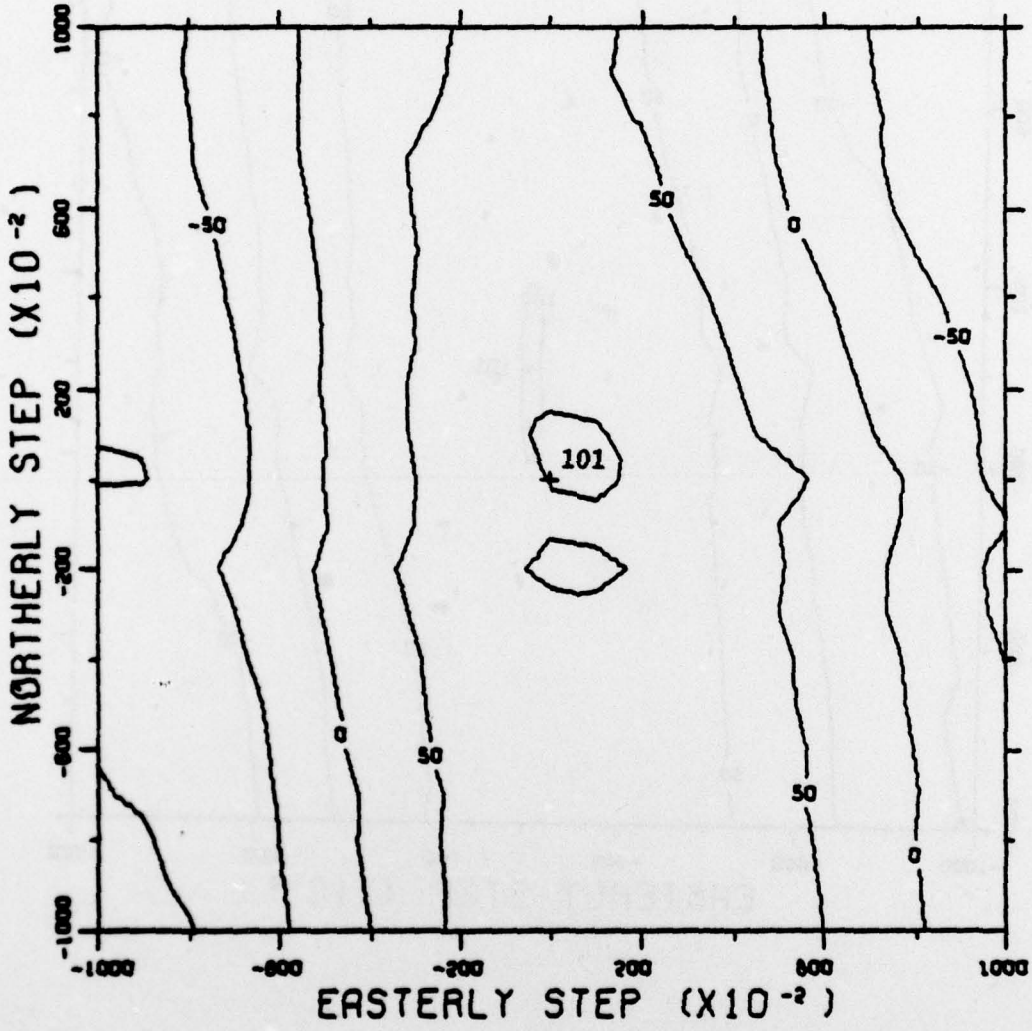

Figure 16: 2-D Cross-covariance Function Between N and Δg (Contour Interval: 50 mgal m)

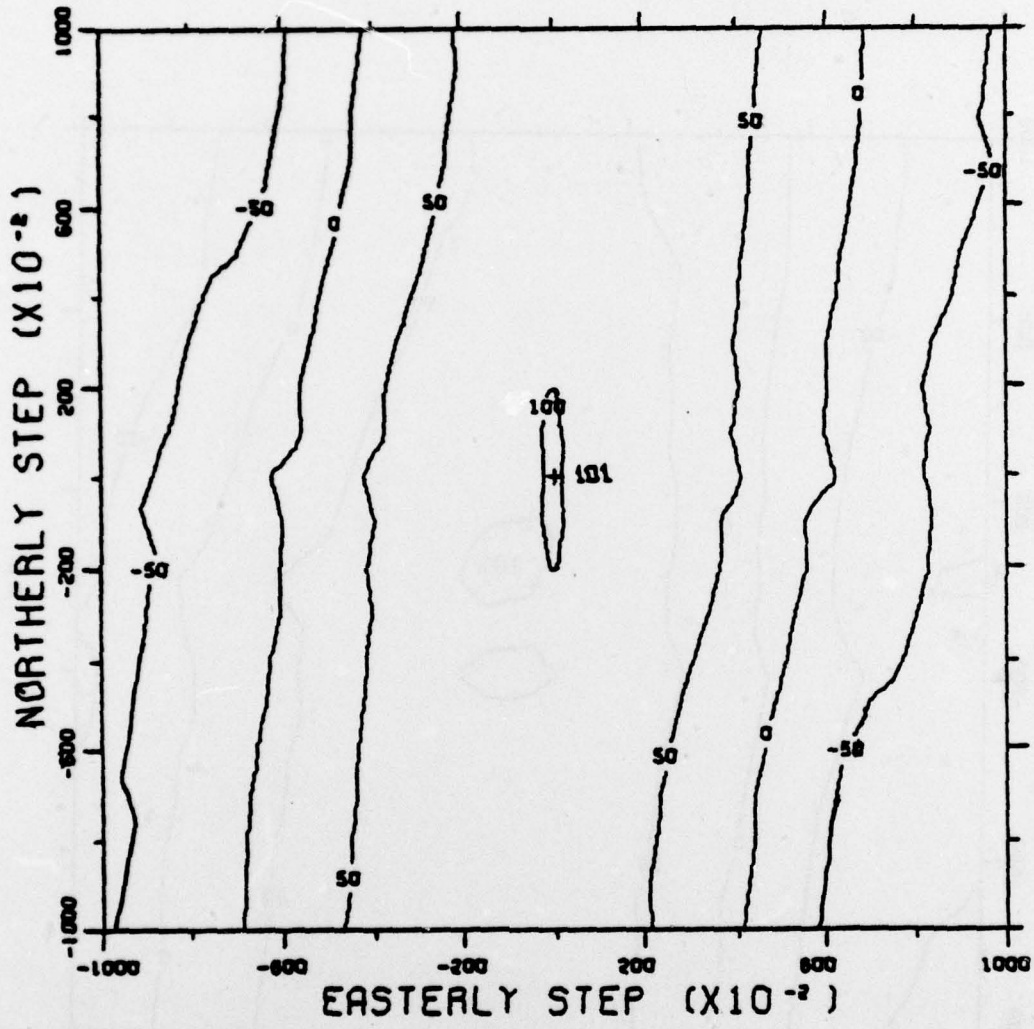

Figure 17: Mean Cross-covariance Function Between N and Δg (Contour Interval: 50 mgal m)

(particularly when viewed against the standard errors of the covariances) it seems reasonable to assume a small decay in the function to assist modelling of the surface.

Jordan (1972, p. 3665) has developed expressions which relate the variances and correlation lengths of the covariance functions for the gravity and undulation data. It would be ideal if such relationships could be used to generate the 2-D covariance functions of all geoidal parameters from (say) the function for Δg using the technique described in section 3.7. Unfortunately, preliminary calculations showed that these theoretical relationships did not describe the actual situation at all well. It may be that this data is not localized enough for such modelling and that it is necessary to use functions more global in nature (e.g. Tscherning and Rapp, 1974).

The modelling of 2-D auto and cross-covariance functions needs further investigation. However, at this stage it was considered more important to discover whether the use of the 2-D functions had any significant effect in collocation. For this reason, discrete data resulting directly from the analysis of the local field was used.

4.3.3 Results of Tests

a) Univariate Predictions: Δg from Δg

For interest, a simple prediction of Δg using the 2-D auto-covariance function was performed, and the results compared with a similar computation using the general covariance analysis (not illustrated). The results are summarized in Table 4 below. Configuration 2 refers to the point arrangement described in Figure 12, and Configuration 3 is described in Figure 17.

Table 4

Summary of Results of Predictions - Data Set 5
(units - $mgal^2$)

Covariance Function	Configuration 2 (population = 228)				Configuration 3 (population = 156)			
	2-D	General	2-D	General	2-D	General	2-D	General
r.m.s. error	15.1	15.2	15.1	15.1	16.3	15.6	21.7*	15.4
m_p	20.1	22.3	19.3	21.4	19.2	22.1	13.0	21.5
$\sum_i a_i$	0.84	0.67	†1.0	†1.0	0.50*	0.79	†1.0	†1.0

† $\sum_i a_i$ forced to 1.0

* see text for comment

Note that the last two columns for both configurations list the results of computations after $\sum a_i$ has been adjusted to unity. Some improvement is noticeable generally in both the r.m.s. error and m_ρ. The exception is the r.m.s. error for the 2-D function in configuration 3 (marked *). Here the r.m.s. deteriorates and individual differences are found to increase by as much as 30 mgal.

The results are in accord with those above (section 4.2). Configuration 3 is symmetrical about the prediction point and the general function produces the superior accuracy. Larger differences occur in the 2-D case where the data is not well represented by the 2-D function (particularly in the SE corner) and this is a big factor in producing the inferior r.m.s. error overall. If the prediction was limited to the regions which displayed the general trend, it appears that because the differences are smaller, the 2-D covariance function would produce the superior results.

The 2-D and general function appear to be equally accurate in the case of Configuration 2. The population for this configuration is large ($\simeq$230) and 15 mgal seems to be the limit of accuracy for this computation. It is noticed that the 2-D function converges more quickly to this limit, suggesting (as does its m_ρ value) a superior accuracy for this covariance function.

b) Multivariate Prediction: N from Δg

The value of N was computed throughout the field from the gravity data by use of equation 2.19, with parameters AX set equal to zero. The gravity points were organized in Configuration 2 for the first test, Configuration 3 for the second. The cross-covariances used to provide the elements of matrix C_{sx} were:

(i) the strict 2-D cross-covariance function shown in Figure 16

(ii) the averaged or symmetric 2-D function (Figure 17), and

(iii) the general cross-covariance function (not illustrated)

This produced three solutions for each of the configurations. The elements of the $\bar{C}$ matrix were taken from Figure 14 for solutions (i) and (ii), and from the general auto-covariance analysis of the gravity for solution (iii).

A histogram of the absolute differences $|v|$ resulting for each solution is shown in Figure 18, and the comparisons of the accuracies achieved are tabulated in Table 5. Note that v is found by differencing the predicted N value from the N value obtained from Figure 13a.

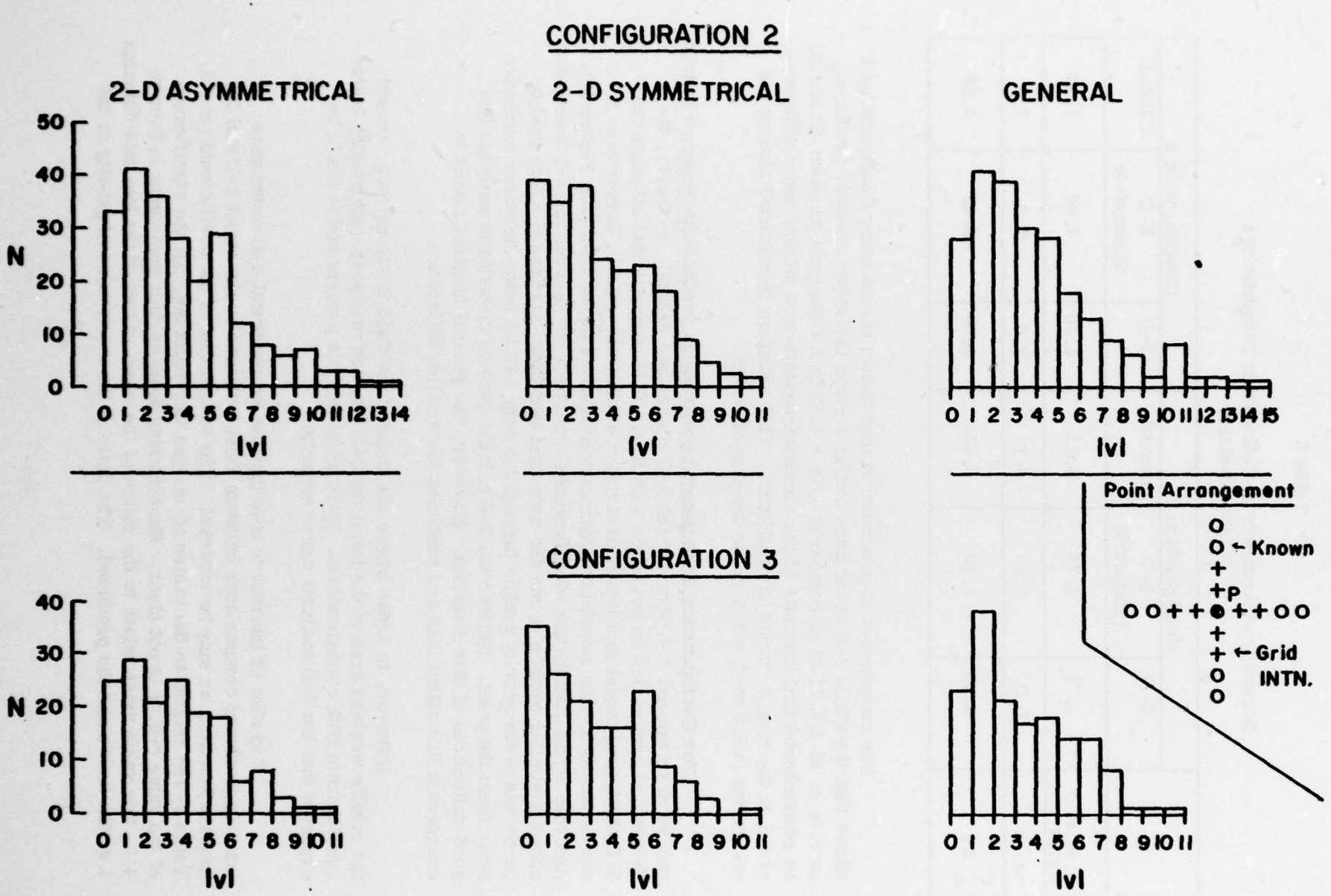

Figure 18: RESULTS OF COLLOCATION TEST COMPUTATIONS

(Units: Meters)

Table 5

Summary of Accuracy of Collocation Computations
(Units : Meters)

	Configuration 2			Configuration 3		
	2-D	2-D Symmetric	General	2-D	2-D Symmetric	General
r.m.s. ± error	4.71	4.74	4.83	4.06	4.00	3.96
m_p ±	8.0	8.0	8.1	7.6	7.8	7.7
$\sum_i a_i$	0.39	0.39	0.45	0.49	0.48	0.53

The comparison of predicted versus known values using Configuration 2 shows that the strict 2-D covariance analysis gives the better results, producing an r.m.s. of ± 4.71 m as compared with ± 4.83 m for the general case. (It should be remembered that the units of the predicted quantity are meters and a difference of 0.1 in the r.m.s. is not insignificant.) This situation is reflected also by the m_p values (± 8.0 m cf ± 8.1 m for the general case).

For Configuration 3 the general covariances produce the superior results (± 3.96 m as against ± 4.06 m for the 2-D covariance values). However, the theoretical accuracies do not agree with this. This suggests that although the 2-D statistical model is a better descriptor of the field overall, larger errors are produced by this model in uncharacteristic areas of the field (see Figure 18). Analysis of the distribution of differences from both the general and 2-D solutions shows a similar pattern exists for both, and that large errors ($|v| > 5$ m) tend to occur where the gravity profile through the computation point increases markedly away from the point. Neither the 2-D nor the general covariance analyses are good reflections of this situation. However, the general function seems to exaggerate this effect less and produces the smaller difference.

However, in areas where the trend of the field is strong (e.g. around the middle western area of the field) the 2-D function produces consistently better results from both configurations. Here anisotropy is present and it would be expected that the 2-D analysis prove superior.

It is also of interest to note that the symmetrical 2-D covariance function produces comparisons between those obtained by the strict 2-D and the general function, as may be expected. The summation of the coefficients (row 3, Table 5) are related to the values of m_p (as they must be), but the significance of the value (≃0.4) is not clear. Generalizing from earlier comments in Section 4.2, this value must relate to the ratios of the mean values of the two data domains i.e. the known and the predicted. The ratio of the mean value of gravity to the

mean value of N in the test area is, in fact, 0.46. However, the relationship noted in the prediction computations between the $\sum a_i$ value and the accuracy does not appear to hold here. That is, the greater accuracy does not necessarily come from that computation whose sum is closer to 0.46.

There is obviously not enough information here to come to any definite conclusions concerning the use of the 2-D function in collocation. Nevertheless, it does seem to follow the pattern noticed from the prediction results. That is, where the anisotropy portrayed by the 2-D covariance analysis is present, the values computed from the 2-D covariances compare more favorably with the known data than do those computed from the general analysis.

5.0 Conclusions

The two-dimensional covariance function provides the most efficient means of detecting and representing the anisotropic characteristics of a data set distributed over a plane. This function graphically describes the covariance which exists between point pairs of all separations and orientations. The extent of anisotropy is indicated by the departure of the contours of the 2-D covariance surface from a circular pattern, and the orientation of the axes of maximum and minimum correlation are clearly shown.

It is possible to model the 2-D covariance surface by generating a simple covariance function for each azimuth, $0 \leq \alpha < 360$. The logarithmic function suggested by Moritz (1976, p. 29) appears to be the best model overall, particularly when the function attains negative values. The fact that the 2-D cross-covariance function is not symmetrical complicates the generation of the surface by this method. It is possible to overcome this problem by using the symmetrical 2-D function to approximate the cross-covariance surface.

The ideal function would enable the generation of all auto and cross-covariance functions knowing the pertinent parameters of (say) the anomalous gravity field. The third-order Markov function suggested by Jordan (1972) has this capability. Unfortunately, the theoretical relationships did not agree with the actual relationships in this instance. It is felt that this is an important area for further research, if the usefulness of the 2-D covariance function is to be fully exploited.

The 2-D covariance function is capable of producing results superior to those obtained by the general function when certain conditions are present. These conditions will produce large differences between elements of the covariance matrices derived from the general covariance analysis and from the 2-D covariance analysis. They will occur when:

(i) anisotropic effects are present and, because of the distribution of the data, predictions must be performed over large separations and in an asymmetric configuration, or

(ii) anisotropy is strongly evident and homogeneous throughout the field. Such an effect can be seen in areas where geoidal slopes are uniformly and consistently large (e.g. the geoid slope across Australia). In fact, under these conditions the solution using the general function appears to break down.

In any case, a 2-D covariance analysis should be performed on data which shows anisotropic tendencies. This will indicate the extent of the azimuth dependence of the covariance function and enable remedial action to be taken (e.g. in the configuration of the data used in subsequent computation) if this appears warranted.

The 2-D covariance surface may also provide useful information concerning a suitable "trend surface" to be fitted to the original data. Knowing that the residuals of the actual data from the trend surface should be isotropic, it should be possible to discover what nature of surface must be fitted in order to transform the 2-D covariance surface to a surface of revolution. (This may be best performed in the spectral domain.) The residuals can then be used in the stochastic processes with the knowledge that they do, in reality possess isotropic characteristics.

6.0 Acknowledgments

I am grateful to Dr. Richard H. Rapp for the opportunity to investigate this topic and for the helpful suggestions and guidance during the course of this research.

References

Agterberg, F. P., "Autocorrelation Functions in Geology", Geostatistics, Plenum Press, New York, 1970.

Blackman, R. B., and J. W. Tukey, The Measurement of Power Spectra, Dover Publications, Inc., New York, 1959.

Brovar, V.V. et al., The Theory of the Figure of the Earth, (Translation), Clearinghouse, #AD608975.

Davis, John C., Statistics and Data Analysis in Geology, John Wiley and Sons, Inc., New York, 1973.

Gaposchkin, E. M. (ed.), Standard Earth III - 1973, Special Report #353, Smithsonian Astrophysical Observatory, 1973.

Grafarend, Erik W., "Geodetic Applications of Stochastic Processes", Physics of the Earth and Planetary Interiors, 12, 1976.

Grafarend, E. and G. Offermans, A Chart of the Deflections of the Vertical in West Germany According to a Geodetically Consistent Kolmogorov-Weiner Model, Deutsche Geodatische Kommission, Series A., Theoretical Geodesy, No. 82, 1975.

Groten, E., Some Numerical Aspects of Least Squares Autoregression Prediction, Fifth Symposium on Mathematical Geodesy, Firenze, 1972.

Groten, E.,"Some Problems of Large Scale Gravity Interpretations", Journal of Geophysics, 41, 1975.

Heiskanen, W. A. and H. Moritz, Physical Geodesy, W. H. Freeman and Co., San Francisco, 1967.

Hirvonen, R. A., On The Statistical Analysis of Gravity Anomalies, Inst. Geod. Phot. Cart., Report No. 19, The Ohio State University, Columbus, 1962.

Hirvonen, R. A., Adjustment by Least Squares in Geodesy and Photogrammetry, Frederick Ungar Publishing Co., New York, 1971.

Holloway, J. L., Jr., "Smoothing and Filtering of Time Series and Space Fields", Advanced Geophys., 4, 1958.

Horton, C. W., W. B. Hempkins and A. J. Hoffman, "A Statistical Analysis of Some Aeromagnetic Maps from the Northern Canadian Shield", Geophysics, Vol. 29, 1964.

Jordan, S. K., Effects of Geodetic Uncertainties on a Damped Inertial Navigation System, International Symposium on Earth Gravity Models and Related Problems, St. Louis, 1972.

Jordan, S. K., "Self-consistent Models for the Gravity Anomaly Vertical Deflections and Undulation of the Geoid", Journal of Geophysical Research, 77, 2, 1972.

Kaula, W. M., "Regression Methods and Non-Uniform Distribution on a Sphere", in Orbital Perturbations from Terrestrial Gravity Data, Contract AF(601)-417, USAF Aeronautical Chart and Information Center, 1966a.

Kaula, W. M., Global Harmonic and Statistical Analysis of Gravimetry, American Geophysical Union Geophysical Monograph Series #9, 1966b.

Kaula, W. M., "Theory of Statistical Analysis of Data Distributed Over a Sphere", Review of Geophysics, Vol. 5, No. 1, 1967.

Kearsley, A. H. W., The Computation of Deflections of the Vertical from Gravity Anomalies, UNISURV Report #S-15, School of Surveying, University of New South Wales, Australia, 1976.

Kubáčková, L., "Disturbance of the Statistical Iostropy of the Gravity Field in the Region of Czechoslovakia's Carpathians", Contrib. Geophys. Inst. Slovak. Acad. Sci. 5, 1974.

Lachapelle, G., Astrogravimetric Levelling by Least Squares Collocation, Contributions of the Graz Group to XVI General Assembly of IUGG/IAG, Grenoble, 1975a.

Lachapelle, G., Predictions of Deviations of the Vertical Using Hetrogeneous Data, Contributions of the Graz Group to the XVI General Assembly of IUGG/IAG, Grenoble, 1975b.

Matheron, G., "Principles of Geostatistics", Economic Geology, Vol. 58, 1963.

Matheron, G., Les Variables Régionalisées et Leur Estimation, Masson et Cie, Paris, 1965.

Miller, K. S., Engineering Mathematics, Dover Publications, New York, 1956.

Monget, J. M., "Une Nouvelle Méthode D' Analyse Statistique Des Données Gravimetriques", Bulletin Geodesique, 94, 1969.

Monget, J. M. and M. Albuisson, "A New Statistical Treatment of Gravity Data", Bulletin Géodesique, 102, 1971.

Moritz, Helmut, Optimal Smoothing of Aerial Gravity Measurements, Department of Geodetic Science Report No. 80, The Ohio State University, Columbus, 1967.

Moritz, Helmut, Advanced Least Squares Methods, Department of Geodetic Science Report No. 175, The Ohio State University, Columbus, 1972.

Moritz, Helmut, Covariance Functions in Least Squares Collocation, Department of Geodetic Science Report No. 240, The Ohio State University, Columbus, 1976.

Nettleton, L. L., Gravity and Magnetics in Oil Prospecting, McGraw-Hill, Inc., New York, 1976.

Rapp, R. H., The Prediction of Point and Mean Gravity Anomalies Through the Use of the Digital Computer, Department of Geodetic Science Report No. 43, The Ohio State University, Columbus, 1964.

Rapp, R. H., Gravity Anomaly Recovery From Satellite Altimetry Data Using Least Squares Collocation Techniques, Department of Geodetic Science Report No. 220, The Ohio State University, Columbus, 1974.

Rapp, R. H., Anomalies Recovered From Geos-3 Altimeter Data Using Least Squares Collocation, Presented at the Spring Annual Meeting of the American Geophysical Union, 1976.

Rapp, R. H. and R. Rummel, Methods for the Computation of Detailed Geoids and Their Accuracy, Department of Geodetic Science Report No. 233, The Ohio State University, Columbus, 1975.

Richardus, P., Project Surveying, North Holland Publishing Co., Amsterdam, 1966.

Smith, G. N., Mean Gravity Anomaly Prediction from Terrestrial Gravity Data and Satellite Altimeter Data, Department of Geodetic Science Report No. 214, The Ohio State University, Columbus, 1974.

Tscherning, C. C., Problems and Results in Least Squares Collocation, Department of Geodetic Science, The Ohio State University, Columbus, 1973.

Tscherning, C. C. and R. H. Rapp, Closed Covariance Expressions for Gravity Anomalies, Geoid Undulations, and Deflections of the Vertical Implied by Anomaly Degree Variance Models, Department of Geodetic Science Report No. 208, The Ohio State University, Columbus, 1974.

Tukey, J. W., "Some Further Inputs", Geostatistics, Plenum Press, New York, 1970.

Vyskocil, V., "On the Covariance and Structure Functions of the Anomalous Gravity Field", Studia Geophysica et Geodetica, Vol. 14, No. 2, 1970.

Whittle, P., "On Stationary Processes in the Plane", Biometrika, 41, 1954.

Wollard, G. P. and K. I. Daugherty, Collection, Processing and Geophysical Analysis of Gravity and Magnetic Data, ACIC Reference Publication 12 (2 Vols.), 1970.

Wollard, G. P. and K. I. Daugherty, Investigations on the Prediction of Gravity in Oceanic Areas, Hawaii Institute of Geophysics, University of Hawaii, 1974.

Wollard, G. P. et al., The Prediction of Gravity in Oceanic Areas, Hawaii Institute of Geophysics, University of Hawaii.

Appendix A1

The angular frequency (ω) and the frequency in cycles per second are related by:

$$f = \frac{\omega}{2\pi}$$

When operating in the spatial domain the time (τ) in equations (3.2) to (3.4) are replaced by the length r. The fundamental wavelength of the signal is assumed to correspond to $m\Delta x$ where m, Δx are defined in equation (3.5). (In the case of data set 1, it is seen that the fundamental wavelength equals 6 grid units, i.e. $m = 6$.)

The frequency associated with the step value r (r also represents the harmonic of the fundamental wavelength) can therefore be expressed as:

$$f_r = \frac{r}{2m\Delta x}$$